MICROCOPY RESOLUTION TEST CHART
NATIONAL BUREAU OF STANDARDS-1963-A

AFGL-TR-84-0083

FIRST- AND SECOND-PHASE GRAVITY FIELD SOLUTIONS BASED ON SATELLITE ALTIMETRY

Georges Blaha

Nova University Oceanographic Center
8000 North Ocean Drive
Dania, Florida 33004

Scientific Report No. 2

January 1984

DTIC

JUN 20 84

AD-A142 256

DTIC FILE COPY

84 06 18 062

REPORT DOCUMENTATION PAGE		READ INSTRUCTIONS BEFORE COMPLETING FORM
1. REPORT NUMBER AFGL-TR-84-0083	2. GOVT ACCESSION NO. ADA.42256	3. RECIPIENT'S CATALOG NUMBER
4. TITLE (and Subtitle) FIRST- AND SECOND-PHASE GRAVITY FIELD SOLUTIONS BASED ON SATELLITE ALTIMETRY		5. TYPE OF REPORT & PERIOD COVERED Scientific Report No. 2
		6. PERFORMING ORG. REPORT NUMBER
7. AUTHOR(s) Georges Blaha		8. CONTRACT OR GRANT NUMBER(s) F19628-82-K-0007
9. PERFORMING ORGANIZATION NAME AND ADDRESS Nova University Oceangraphic Center 8000 North Ocean Drive Dania, Florida 33004		10. PROGRAM ELEMENT, PROJECT, TASK AREA & WORK UNIT NUMBERS 61102F 2309G1BB
11. CONTROLLING OFFICE NAME AND ADDRESS Air Force Geophysics Laboratory Hanscom AFB, Massachusetts 01731 Contract Monitor: George Hadgigeorge/LWG		12. REPORT DATE January 1984
		13. NUMBER OF PAGES 111
14. MONITORING AGENCY NAME & ADDRESS(if different from Controlling Office)		15. SECURITY CLASS. (of this report) Unclassified
		15a. DECLASSIFICATION/DOWNGRADING SCHEDULE

16. DISTRIBUTION STATEMENT (of this Report)

Approved for public release; distribution unlimited.

17. DISTRIBUTION STATEMENT (of the abstract entered in Block 20, if different from Report)

18. SUPPLEMENTARY NOTES

19. KEY WORDS (Continue on reverse side if necessary and identify by block number)

Satellite altimetry	Least-Squares adjustment	Variance-covariances
Surface tide	Spherical Harmonics	Residuals
Ocean tide	Point masses	Collocation with noise
Bottom tide	State vectors	Errorless collocation

20. ABSTRACT (Continue on reverse side if necessary and identify by block number)

The increasing accuracy of satellite altimetry and its growing use in the determination of the general circulation of the oceans provide the motivation for conceiving the most rigorous model possible in relating the pressure and geopotential gradients. In response to such a need, the standard derivation is refined through the inclusion of second-order effects. This refinement is carried out with the extensive use of tensor notations. →word

DD FORM 1473 1 JAN 73   EDITION OF 1 NOV 65 IS OBSOLETE

Since altimeter measurements are directly affected by the surface (geocentric) tide, an exact representation of the latter is important. An improvement of the altimeter model with tidal effects included is achieved by an adaptation of Schwiderski's formula giving the ocean bottom deformation due to ocean tidal loading. The resulting model for the bottom tide and, especially, for the surface tide can be used in conjunction with all of the tidal constituents.

Due to an imperfect description of the earth's gravity field by a truncated spherical-harmonic series in a first-phase adjustment process, the neglected effect is superimposed on the altimetric noise and acts as if increasing its variance and introducing covariances in a global sense. This added effect can be evaluated using the geoidal covariance function. The total effect (including the noise proper), when treated as the first-order autoregressive process, yields a highly patterned variance-covariance matrix whose inverse is a tri-diagonal matrix. The latter is used here as the weight matrix of observations in a least-squares adjustment, offering almost the same computer economies as a diagonal weight matrix when compared to the rigorous, fully populated weight matrix. However, the errors associated with a diagonal weight matrix are greatly reduced in this approach.

The point-mass adjustment model, based on the residuals from the spherical-harmonic adjustment of satellite altimetry, has been recently modified to allow for an efficient, large-scale resolution of the geoidal detail. That task has been accomplished with the aid of an algorithm resulting in a banded system of normal equations. However, the point-mass model has not included any tidal effects. In the present analysis this model is extended, in the sense that certain tidal parameters, associated with a given ocean basin, are adopted as adjustable quantities. In a least-squares adjustment encompassing such a basin the new set of parameters is common to every observation and leads thus to a full border portion of the matrix of normal equations. This results in a banded-bordered system of normal equations which can be resolved almost as efficiently (due to a relatively small number of tidal parameters) as the above banded system.

As an alternative to the point-mass adjustment (without tidal parameters), an approach is presented which is an adaptation of the collocation theory. First, the standard prediction formulas corresponding to the least-squares collocation with noise are recapitulated, yielding the "unsmoothed" geophysical quantities based on the unaltered signal and noise at every observation point. Subsequently, these formulas are modified to yield "smoothed-out" geophysical quantities. Here a part of the signal, representing the (fine) gravity field variations beyond the desired smoothing level, is pushed into the realm of "noise". The standard collocation approach is unchanged except that during the formation of the first matrix in the prediction formula, the covariance (or cross-covariance) function is no longer utilized in conjunction with the expansion degree "∞", but only in conjunction with the degree corresponding to the required smoothness. Finally, the (pure) densification of the predicted geophysical quantities in view of contour maps can be carried out efficiently via the errorless collocation. Consistent with this procedure, the residuals at observation points computed with respect to the geoidal contour map can also be obtained using the errorless collocation.

TABLE OF CONTENTS

TABLE OF CONTENTS (Continued)

LIST OF FIGURES

LIST OF TABLES

v

A-1

1. INTRODUCTION

This report pursues the development of satellite altimeter adjustment model based on the short-arc algorithm. In the first-phase gravity field adjustment the data consist of altimeter observations, the smoothed surface approximating the geoid is described by a truncated set of spherical-harmonic potential coefficients, and each satellite arc is described by six state vector components. In addition, certain tidal effects can also be included in the adjustment. As can be gathered from [Blaha, 1982], each diurnal and semidiurnal tidal constituent considered is attributed two adjustable parameters, a global amplitude factor and a global phase angle correction.

The altimeter residuals can be used in the role of data in a second-phase solution concerned with a more detailed description of the earth's gravity field. The report [Blaha, 1983] makes use of point-mass parameters in the second-phase adjustment which yields a banded system of normal equations resolved through the application of the "modified Choleski algorithm". Due to the nature of this algorithm, the geoid over entire ocean basins can be adjusted in a few overlapping strips of point masses, leading to a detailed resolution of the oceanic geoid and the related geophysical quantities on a global basis.

The material contained in the present report can be divided into four categories. The first category is concerned with improvements in the model of the sea surface and of tidal effects; the second category is concerned with an improvement in weights attributed to altimeter observations in the

first-phase adjustment; the third category is concerned with a second-phase adjustment which, however, includes also the chosen tidal parameters as adjustable quantities; and the fourth category is concerned with an application of the least-squares collocation with noise to a second- or third-phase resolution of the earth's gravity field.

When dealing with various ocean-surface characteristics (first category above), one recognizes that the relationship between the pressure and geopotential gradients in the ocean has important oceanographic, meteorological and geodetic applications. With regard to the usual meteorological practice, for example, such a relationship leads to the elimination of the need for the variation of density with elevation when expressing the geostrophic wind equations on an isobaric surface. The point to be emphasized here is that the above gradient relationship is paramount to solving important geodetic and oceanographic problems, such as the determination of the departures of the standard ocean from the geoid. Without taking it properly into account one could not avoid discrepancies between altimetric and oceanographic solutions of the sea surface. The refinement of the usual formula giving this relationship is the topic of Chapter 2.

Since the altimeter measurements are directly affected by the surface (geocentric) tide, an exact representation of the latter is important. The improvement of the overall tidal model in its relation to satellite altimetry is thus linked to the improvement of the model for the bottom tide which, when added to the ocean tide, yields the surface tide. This topic (also belonging to the first category) is addressed in Chapter 3.

Due to an imperfect description of the earth's gravity field and its

fundamental surface, the geoid, by a truncated spherical-harmonic series in a first-phase adjustment, the neglected effect is superimposed on the observational noise and acts as if increasing its variance and introducing covariances in a global sense. The temptation is great to use this new variance, and to neglect the geoidal covariances. The advantage achieved with such a simplification is the elimination of the weight matrix of observations from the least-squares algorithm. The price to pay for this economical gain is a less rigorous adjustment. A compromise solution offering almost equally significant computer economies is presented in Chapter 4 (complemented by Appendix 1).

The "modified Choleski algorithm" developed in [Blaha, 1983] is based on three separate steps: 1) elimination of the point masses from an observation equation if they are sufficiently far from the pertinent observation point, 2) special arrangement of the point-mass parameters in the adjustment scheme, and 3) resolution of the resulting system through an adaptation of the well-known Choleski algorithm. However, this approach does not provide for an additional, second-phase adjustment of tidal parameters which may be desirable at the level of individual ocean basins. The task of including chosen tidal parameters in the second-phase adjustment of point masses is addressed in Chapter 5.

A second-phase adjustment in terms of parameters such as the point masses requires the formation of normal equations and their resolution in a simultaneous least-squares process. This process can be computationally demanding, even if no tidal parameters are present and if advantage is taken of the "modified Choleski algorithm". An equivalent second-phase approach can be

-3-

developed in using an adaptation of Moritz's [1980] least-squares colloca-
tion with noise.   This approach can also serve in predicting other geophy-
sical quantities in addition to geoid undulations, such as gravity anomalies.
It is described in Chapter 6 together with Appendices 2 and 3.

2. RELATIONSHIP BETWEEN THE PRESSURE AND GEOPOTENTIAL GRADIENTS IN THE OCEAN DERIVED IN TENSOR NOTATIONS

The increasing accuracy of satellite altimetry and its growing use in the determination of the general circulation of the oceans provide the motivation for conceiving the most rigorous model possible in relating the pressure and geopotential gradients. It is deemed worthwhile, then, to refine the standard derivation appearing e.g. on pages 187-189 in [Hess, 1959] by including what could be termed "second-order effects". Even if these effects proved insignificant for the current and near-term prospects, it is reassuring to know the extent of approximations entering the model used in the actual applications.

This chapter focuses on the derivation of the refined gradient formula in curvilinear coordinates with the aid of tensor notations. 't then proceeds to the simplification removing the second-order effects, which results in the standard formula as presented in the above reference. The differences between these two formulations are discussed in the closing paragraphs.

The problem to be addressed is depicted in Figure 1. The figure displays the curvilinear nature of the coordinates associated with the point Q (at the intersection of the two planes shown), although the W-coordinate line through Q' has also been drawn. In solving the problem at hand, some elements of tensor analysis as presented by Hotine [1969] will be used.

The coordinate system employed is symbolized by x^r, r=1,2,3. Here the third space coordinate is $x^3 \equiv W$, the geopotential; x^1 and x^2 are surface

-5-

coordinates, where the surface is W = constant, as well as the other two space coordinates. Accordingly, $x^r \equiv (x^1, x^2, W)$. As one example, x^1 and x^2 could be the geodetic latitude and longitude, respectively.

In accordance with the geodetic convention, the potential is taken as increasing downward. If the infinitesimal vector "dx" associated with the point Q and represented by its contravariant components dx^r should lie in the surface W = constant, then along its direction one has

$$dW \equiv (\partial W/\partial x^r)dx^r \equiv W_r dx^r = 0 .$$

Thus W_r, the gradient of W, is a covariant vector perpendicular to the surface W = constant. If ν_r represents the covariant components of the (downward) unit-vector "ν" perpendicular to this surface at Q, the above finding is formalized as

$$W_r = g \, \nu_r , \tag{2.1}$$

where g, the gravity at Q, is the magnitude of W_r.

If ds is the length along ν so that the contravariant infinitesimal vector considered is $\nu^r ds$, then along this direction we have

$$dW = W_r \nu^r ds ,$$

and due to (2.1),

$$dW = g \, ds , \tag{2.2}$$

which is the familiar geodynamic equation.

Figure 1

Schematic representation of the surfaces W = constant and P = constant, where W is the geopotential and P is the pressure in the standard ocean.

The coordinates of only four (out of six) points depicted in the figure are written explicitly. In general, the zero coordinates could be replaced by the pertinent $x^1_{(Q)}$, $x^2_{(Q)}$ and $W_{(Q)}$.

So far the coordinate system considered is quite general and the direction of the W-coordinate line (along which x^1 and x^2 are constant) does not have to coincide with ν. This statement applies to Q or any other point in the surface W = constant. The x^1- and x^2- coordinate lines, on the other hand, lie in this surface. Thus the W-coordinate line is not, in general, perpendicular to x^1- or x^2-lines at Q or any other point of the surface.

Consider now the infinitesimal neighborhood of Q in space. Along the x^1-, x^2- and W-coordinate lines we have, respectively:

$$dx^r_{(1)} \equiv (dx^1, 0, 0) \ , \quad dx^r_{(2)} \equiv (0, dx^2, 0) \ , \quad dx^r_{(3)} \equiv (0, 0, dW).$$

(2.3)

In terms of Figure 1, the length elements of these infinitesimal vectors are $d\ell_{(i)}$, i=1,2,3. From the basic relation $d\ell^2 = g_{rs} dx^r dx^s$ giving the square of the length element along any vector dx, where g_{rs} is the metric tensor at Q, one finds

$$d\ell_{(1)} = \sqrt{g_{11}} \, dx^1 \ , \quad d\ell_{(2)} = \sqrt{g_{22}} \, dx^2 \ , \quad d\ell_{(3)} = \sqrt{g_{33}} \, dW \ .$$

Since, in general, the contravariant components of the unit vector in the direction of dx are $\ell^r = dx^r/d\ell$, we have for the unit vectors $\ell_{(i)}$ in the above directions:

$$\ell^r_{(1)} = (1/\sqrt{g_{11}}, 0, 0) \ , \quad \ell^r_{(2)} = (0, 1/\sqrt{g_{22}}, 0) \ , \quad \ell^r_{(3)} = (0, 0, 1/\sqrt{g_{33}}) \ .$$

(2.4)

These formulas are valid regardless of the nature of the coordinate system.

Associated with the interval QQ' of Figure 1, we denote

$$dx^r \equiv (dx^1, dx^2, 0) \; , \tag{2.5}$$

$$d\ell = [g_{11}(dx^1)^2 + g_{22}(dx^2)^2 + 2g_{12}dx^1dx^2]^{1/2} \; ,$$

$$\ell^r = (dx^1/d\ell, dx^2/d\ell, 0) \; . \tag{2.6}$$

Since x^α, $\alpha=1,2$, are space as well as surface coordinates, it holds true that $g_{\alpha\beta} = a_{\alpha\beta}$, where $a_{\alpha\beta}$ is the surface metric tensor. In the (x^1, x^2, W) coordinates one has $W_r = (0,0,1)$; thus, due to (2.1), the unit vectors $\ell_{(1)}$, $\ell_{(2)}$ and ℓ are confirmed to lie in the surface W = constant.

Next introduce normal coordinates so that the pertinent infinitesimal vectors, which are here split naturally according to their coordinate differences as

$$(dx^1, dx^2, dW) = (dx^1, dx^2, 0) + (0, 0, dW) \; , \tag{2.7}$$

be at the same time conveniently split into a vector lying in the surface W = constant and a vector perpendicular to it. The coordinates x^1 and x^2 can still be quite general. For example, they could again be the geodetic latitude and longitude, respectively, but they would have such characteristics only on one surface, in this case the above surface W = constant. This transpires from the paragraph 8 on page 104 in [Hotine, 1969], where such a surface is called "base surface".

In the normal coordinate system (x^1, x^2, W) the metric tensor can be written in the abbreviated form as

$$g_{rs} = (g_{\alpha\beta}, 1/g^2) \; , \tag{2.8}$$

-9-

similar to equation (15.03) in [Hotine, 1969]. This means that in the matrix form of g_{rs} the elements (1,3), (2,3) and (3,1), (3,2) are zero. Since $t_r = g_{rs}t^s$ holds true for any vector t, it now follows from (2.4) that

(2.9)

$$\ell_{(1)r} = (\sqrt{g_{11}}, g_{12}/\sqrt{g_{11}}, 0), \quad \ell_{(2)r} = (g_{12}/\sqrt{g_{22}}, \sqrt{g_{22}}, 0), \quad \ell_{(3)r} = (0,0,1/g),$$

where $g_{33} = 1/g^2$ has been taken into account. Upon contractions of (2.9) with (2.4) and (2.6), it is verified that the unit vector $\ell_{(3)}$ is perpendicular to the unit vectors $\ell_{(1)}$, $\ell_{(2)}$ and ℓ. We thus have

$$\nu_r \equiv \ell_{(3)r} = (0,0,1/g) \,, \qquad \nu^r \equiv \ell^r_{(3)} = (0,0,g) \,, \tag{2.10}$$

$$ds \equiv d\ell_{(3)} = dW/g \,. \tag{2.11}$$

Upon denoting the vector along QT' as dx', where T' lies in the surface P=constant, this vector can be split, according to (2.7), as

$$dx'^r = dx^r + dx^r_{(3)} \,, \tag{2.12}$$

where $dx'^r \equiv (dx^1, dx^2, dW)$ corresponds to QT' as just stated, $dx^r \equiv (dx^1, dx^2, 0)$ corresponds to QQ' (see equation 2.5), and $dx^r_{(3)} \equiv (0,0,dW)$ corresponds to QT (see equation 2.3). According to the foregoing, dx lies in the surface W = constant and $dx_{(3)}$ is perpendicular to it. All three vectors dx', dx and $dx_{(3)}$, whose length elements in Figure 1 are $d\ell'$, $d\ell$ and $d\ell_{(3)}$, respectively, are associated with Q.

Consider the change in W from Q to T', namely

$$dW_{QT'} = W_r dx'^r = W_r dx^r + W_r dx^r_{(3)} \,.$$

The first term on the right-hand side is zero due to the relation preceding (2.1). In consulting (2.2) and the equation that preceded it, the second term with $dx^r_{(3)} \equiv \nu^r ds \equiv \ell^r_{(3)} d\ell_{(3)}$ leads to

$$dW_{QT'} = g\, d\ell_{(3)} \quad . \tag{2.13}$$

Next consider the change in P from Q to Q'. Due to

$$dP_{QT'} = P_r dx'^r = P_r dx^r + P_r dx^r_{(3)} = 0 \quad ,$$

it follows that

$$dP_{QQ'} = P_r dx^r = -P_r dx^r_{(3)} \equiv -dP_{QT} \quad .$$

However, the hydrostatic equation for the compressible standard ocean at Q yields

$$dP_{QT} = g\, \rho\, d\ell_{(3)} \quad , \tag{2.14}$$

where ρ is the water density at Q, due to the fact that $d\ell_{(3)}$ is the displacement in the direction of gravity (i.e., perpendicular to the equipotential surface W = constant). Accordingly,

$$dP_{QQ'} = -g\, \rho\, d\ell_{(3)} \quad . \tag{2.15}$$

In combining (2.13) and (2.15), we have

$$dW_{QT'} = -(1/\rho)dP_{QQ'} \quad , \tag{2.16}$$

specifying the change in geopotential along an isobaric surface in terms of the change in pressure along an equipotential surface. Next we address

the problem of the rate of change in these quantities along the respective paths.

The following relations are obtained from (2.13) and (2.15), respectively:

$$\partial W / \partial \ell' = g(d\ell_{(3)} / d\ell') , \tag{2.17}$$

$$\partial P / \partial \ell = -\rho g(d\ell_{(3)} / d\ell) . \tag{2.18}$$

These equations yield

$$\left. \begin{array}{l} \partial W / \partial \ell' = -(1/\rho) \, f \, \partial P / \partial \ell , \\[2mm] \qquad f = d\ell / d\ell' . \end{array} \right\} \tag{2.19}$$

From the formula $d\ell'^2 = g_{rs} dx'^r dx'^s$, where g_{rs} is given in (2.8) and dx'^r is given following (2.12), one obtains

$$d\ell' = [d\ell^2 + (dW/g)^2]^{1/2} \equiv (d\ell^2 + d\ell_{(3)}^2)^{1/2} , \tag{2.20}$$

where $d\ell$ appears in the relations following (2.5) and $d\ell_{(3)}$ appears in (2.11).

From (2.19) and (2.20), one writes

$$f = (1 + d\ell_{(3)}^2 / d\ell^2)^{-1/2} \equiv [1 + (dW/g)^2 / d\ell^2]^{-1/2} . \tag{2.21}$$

If the two surfaces are "close" to each other, in the sense that

$$d\ell_{(3)} \equiv dW/g \ll d\ell ,$$

then the approximations

-12-

$$f = 1 \, , \qquad \Big\}$$
$$\partial W/\partial \ell' = -(1/\rho)\partial P/\partial \ell \, , \quad \Big\} \qquad\qquad (2.22)$$

are satisfactory. In this context one can regard the pressure gradient along equipotential surfaces as interchangeable with the geopotential gradient along isobaric surfaces (except for a factor), a classical oceanographic procedure.

When comparing equation (2.22) with the corresponding equations in [Hess, 1959] (it precedes equation 12.10 therein and will be designated by the symbol "*"), we notice the difference in sign. However, this stems from the orientation of the z-axis in * (positive upward) as opposed to the distance $d\ell_{(3)}$ taken here as positive downward. If, in the above reference, one stipulated that $dW = -gdz$ for W increasing downward in agreement with the geodetic convention, the difference in sign would disappear.

The equivalent of * can be obtained upon dividing both sides of equation (2.16) by $d\ell$. The left-hand side of this new equation becomes the geopotential gradient along an isobaric surface, $\partial W/\partial \ell'$, if we assume that $d\ell \equiv d\ell'$. With this approximation the new equation is then (2.22). Clearly, a simplification of this kind makes the rigorous formulation (2.19) and the practical formulation (2.22) indistinguishable. Thus the standard derivation leading to * causes the rigorous gradient model (2.19) with f given by (2.21) to remain hidden. As we have seen, such a relationship can be unearthed if one considers the gravity-related (curvilinear) coordinate system and focuses on its W-coordinate.

3. IMPROVED FORMULATION OF THE SURFACE TIDE IN THE SATELLITE ALTIMETRY ADJUSTMENT MODEL

The altimeter measurements are directly affected by the surface (geocentric) tide. Since the surface tide is given by the addition of the ocean tide and the bottom tide, an exact representation of the latter is important. However, when the tidal adjustment was formulated in [Blaha, 1982], certain approximations were adopted, such as

$$-u_\ell \simeq 0.06\xi \ \dots\dots \ M_2 \text{ constituent },$$
$$-u_\ell \simeq 0 \quad \dots\dots \ \text{all the other diurnal and semidiurnal constituents },$$

$$(3.1)$$

where u_ℓ, a part of the bottom tide, is the ocean bottom deformation due to the ocean tidal loading and ξ is the ocean tide. These approximations were made through the inspections and comparisons of tidal contour maps, especially those pertaining to the M_2 tide (see pages 97-106 of [Estes, 1980] and pages 386-402 of [Parke and Hendershott, 1980]).

In using (3.1), the following model was formulated on page 56 of [Blaha, 1982] for the diurnal and semidiurnal constituents identified by the index j:

$$h_j = c'\xi_j + h \times (\text{equilibrium tide})_j ,$$

$$(3.2a)$$

where

$$c' = 0.94 \ \dots\dots \ M_2 \text{ constituent,}$$
$$c' = 1.00 \ \dots\dots \ \text{the other diurnal and semidiurnal constituents,}$$
$$h = 0.61, \text{ a Love number,}$$

$$(3.2b)$$

and where

    h_j = surface tide for the constituent j ,

    ξ_j = ocean tide for the constituent j .

The surface tide was considered in the above reference on pages 39-42, where it was denoted as ξ_s .

An improvement in the above model can be achieved by adopting a more complex tidal model developed by Schwiderski [1980], where

$$\xi^b = \xi^e + \xi^{eo} , \tag{3.3}$$

with

    ξ^b = bottom tide,

    ξ^e = earth tidal elevation expressed as 0.61η, η being the Newton's equilibrium tide and 0.61 being the Love number h,

    ξ^{eo} = earth-dip response to oceanic tidal load.

The tidal model has been further refined in Schwiderski's recent NSWC reports concerned with the global ocean tides. Although these reports do not deal with the altimeter adjustment per se, certain features of the tidal model presented therein can have a beneficial effect on the global adjustment model of satellite altimetry.

In particular, the following improved relationships developed by Schwiderski can be used with advantage:

$$\xi^e = 0.612\eta , \tag{3.4a}$$

$$\xi^{eo} = -0.0667\xi. \tag{3.4b}$$

Equation (3.4b) provides an improved formula for the ocean bottom deformation due to ocean tidal loading, written as

$$-u_\ell = 0.0667\xi \ , \tag{3.4b'}$$

which can be used in conjunction with all of the tidal constituents. Combined with (3.3), equations (3.4a,b) imply that

$$\xi^b = 0.612\eta - 0.0667\xi \ . \tag{3.5}$$

Due to

$$\xi^s = \xi + \xi^b \ ,$$

where ξ^s is the surface tide (in [Blaha, 1982] s and b were used as lower indices), it follows that

$$\xi^s = 0.9333\xi + 0.612\eta \ . \tag{3.6}$$

The final formula (3.6) can be used in conjunction with all the constituents, long-period as well as diurnal and semidiurnal. In the notations of [Blaha, 1982], it can be transcribed as

$$h_j = c'\xi_j + h \times (\text{equilibrium tide})_j \ , \tag{3.7a}$$

which has the same form as (3.2a), but where

$$\left.\begin{array}{l} c' = 0.9333 \ \ldots\ldots \ \text{all of the tidal constituents,} \\[1em] h \ = 0.612, \text{ a Love number.} \end{array}\right\} \tag{3.7b}$$

-16-

The improvement achieved with the refined model can be assessed by comparing (3.7b) with (3.2b). The change in the value of h is of little consequence. However, the change affecting the M_2 constituent is more important as are the changes affecting the other diurnal and semidiurnal constituents (the relative changes affecting the latter are greater than the relative change in M_2 , but this relationship does not necessarily hold true for the absolute changes in the geocentric distance). Due to the changes in c' above, the partial derivatives with respect to all the diurnal and semidiurnal constituents are modified as well.

The long-period constituents have been treated in [Blaha, 1981, 1982] in a simplified model, where the ocean tidal loading as well as other effects were disregarded. The model was based on a modified equilibrium tide since no spherical-harmonic tidal coefficients were available to express the ocean tide ξ_j for these constituents. However, this situation may change due to Schwiderski's recent reports offering a possibility to derive such coefficients and thus to treat some or all of the long-period constituents Mf, Mm and SSa in the same fashion as the diurnal and semidiurnal constituents above, i.e., via equations (3.7a,b). We can close this discussion by stating that the modifications (3.7b) represent an improvement of the tidal adjustment model expected to be translated into an improvement in satellite altimetry results by several centimeters, especially in the tidal effects themselves and in the altimetry residuals.

4. WEIGHTING SCHEME FOR A GLOBAL ADJUSTMENT OF SATELLITE ALTIMETRY

The data in satellite altimetry consist of altimeter observations whose noise level has been reduced, in the case of SEASAT, to 0.1-0.2m. The global (first-phase) adjustment model provides for a simultaneous least-squares solution of a truncated set of spherical-harmonic (S.H.) potential coefficients, the state vector (s.v.) parameters on all satellite arcs and, optionally, certain tidal parameters. However, due to an imperfect description of the earth's gravity field and its fundamental surface, the geoid, by a truncated series, the neglected effect will be superimposed on the observational noise and act as if increasing its variance and introducing covariances in a global sense. Therefore, if the altimeter observations were treated as independent and as having the one-sigma level of 0.1-0.2m, they would largely override any conflicting information supplied by the weighted S.H. coefficients and, especially, the weighted s.v. parameters. The problem would be further compounded by high density of geoidal data.

The last statement can be corroborated by the realization that the geoid represents a smooth function and the participation of a great number of observations short distances apart would lead to a similar overall effect on the above parameters (the observations treated as independent would be allowed to unduly reinforce each other). This effect can be inferred from the geoidal covariance function constructed for a given truncation level, allowing quantitative evaluations of both the geoidal variances at single points and the geoidal covariances for pairs of points separated by given distances. The lower the degree and order truncation, the larger these numbers and the smoother the covariance function.

-18-

The first-phase adjustment at AFGL is performed in terms of a (14,14) truncated set of S.H. potential coefficients. The covariance function can be used here to quantify the overall effect of the neglected coefficients, from degree $n = 15$ onward (in theory, to infinity; in practice, to $n = 500$ or $n = 1,000$, etc.). This effect can be represented by the one-sigma level, i.e., the square-root of the geoidal variance, which for the (14,14) truncation has been computed as 4.9m. However, in using SEASAT observations this quantity is estimated as 3.2m; the procedure giving this estimate will be presented later. Combining this value with the 0.1-0.2m sigma of the observational noise proper still yields about 3.2m. Even though the total input sigma is thus made substantially higher than 0.1-0.2m, the neglect of the geoidal covariances could still be detrimental to the adjustment in the above sense of undue reinforcement of observations. But the temptation to neglect the geoidal covariances is great from the practical standpoint. The significant advantage achieved with such a simplfication is the elimination of the weight matrix of observations from the least-squares algorithm (more precisely, the reduction of a fully populated weight matrix for each satellite arc to a constant times the unit matrix). A compromise solution offering almost equally significant computer economies will be presented in this chapter.

The proper treatment of altimeter observations would consist in filling the input variance-covariance matrix with the values obtained through the use of the geoidal covariance function and termed "rigorous". In choosing this avenue, one would be faced with the task of inverting one such matrix per satellite arc, or pre-inverting such matrices according to the number of

observations. If all the arcs had the same number of observations -- such as 54 at 0.5^0 intervals making up for about 26^0 arcs at seven-minute durations which has been the upper limit adopted for SEASAT -- only one pre-inverted matrix (the weight matrix P) would be needed. However, this is not the case in practice. The subsequent formation of normal equations with the fully populated weight matrix would represent further requirements compared with the simplified approach of neglected covariances. For example, a greatly increased computer storage would be needed because the whole design matrix (A) of observation equations for an arc would have to be retained in the active memory. Its dimensions are (m×u), m being the number of observations and u being the number of parameters. In the simplified approach only one row of this matrix is needed at a time. With regard to the computer run-time during the formation of the matrix of normal equations associated with that arc, the number of scalar multiplications would also increase significantly in such a comparison, from mu^2 in the simplified approach to $mu^2 + m^2u$ in the "rigorous" approach.

4.1 First-Order Autoregressive Process

A compromise solution will now be addressed, promising from both the accuracy and the economy standpoints. The input variance-covariances will be slightly modified from their "rigorous" values as represented by the geoidal covariance function. As a result, a highly patterned tri-diagonal weight matrix known beforehand will become available. This "modified approach" corresponds essentially to the first-order autoregressive process described in [Brown and Trotter, 1969]. In the same reference, the second-order autoregressive process would correspond to a five-diagonal weight matrix, etc. In the case at hand, the tri-diagonal weight matrix is arrived at via slight deformations of the original covariance function. In particular, if the covariance function becomes of the form yielding the following variance-covariance matrix,

$$
C = \sigma^2 \begin{bmatrix}
1 & \rho & \rho^2 & \rho^3 & \ldots & \rho^{m-1} \\
\rho & 1 & \rho & \rho^2 & \ldots & \rho^{m-2} \\
\rho^2 & \rho & 1 & \rho & \ldots & \rho^{m-3} \\
\vdots & & & & & \\
\rho^{m-1} & \rho^{m-2} & & & \ldots & 1
\end{bmatrix},
\tag{4.1}
$$

then the weight matrix follows as

$$P \equiv C^{-1} = \{1/[\sigma^2(1-\rho^2)]\} \begin{bmatrix} 1 & -\rho & 0 & 0 \ldots\ldots & 0 & 0 & 0 \\ -\rho & 1+\rho^2 & -\rho & 0 \ldots\ldots & 0 & 0 & 0 \\ 0 & -\rho & 1+\rho^2 & -\rho \ldots\ldots & 0 & 0 & 0 \\ \vdots & & & & & & \\ 0 & 0 & \ldots\ldots\ldots\ldots & -\rho & 1+\rho^2 & -\rho \\ 0 & 0 & \ldots\ldots\ldots\ldots & 0 & -\rho & 1 \end{bmatrix}, \quad (4.2)$$

as can be verified upon pre- or post-multiplying C by P.

Clearly, when passing from the diagonal (simplified) to the tri-diagonal (modified) case, the increases in the storage requirements and in the number of scalar multiplications are negligible when compared to the increases associated with the "rigorous" case. Furthermore, the pattern in (4.2) is the same regardless of the dimensions of P so that no separate inversions, or storage of pre-inverted matrices, are necessary for m varying from arc to arc, unlike in the "rigorous" case. Yet, the tri-diagonal case yields the solution which is likely to closely approximate the "rigorous" solution, much more so than could be expected from the diagonal case. This depends, of course, on how much the covariance function is to be deformed in order to fit the tri-diagonal scheme. A simple procedure of arriving at the tri-diagonal case is presented in the sections below. The analysis will be concluded with a special example showing the improvement represented by the tri-diagonal case versus the diagonal case.

4.2 Geoidal Covariance Function

The representation of the covariance function for geoid undulations is based on the results of [Tscherning and Rapp, 1974]. These results were adapted in [Blaha, 1982] to give the k-degree variance (in meters square) as follows:

$$\sigma_k^2 = 17,981 \times 0.999617^{k+2}/[(k-1)(k-2)(k+24)]. \tag{4.3}$$

The covariance function for geoid undulations is then given as

$$D(\psi) \equiv M\{N,N'\} = \sum_{k=3}^{\infty} \sigma_k^2 \, P_k(\cos\psi) \, ,$$

where the operator M indicates averaging over the whole unit sphere, N and N' are the geoid undulations at any two points P and P' separated by the spherical distance ψ, and $P_k(\cos\psi)$ are the Legendre polynomials in the argument $\cos\psi$. The covariance function corresponding to the bandwidth n_1 through n_2 would read

$$D'(\psi) = \sum_{k=n_1}^{n_2} \sigma_k^2 \, P_k(\cos\psi) \, ,$$

whereas the covariance function corresponding to the truncation n can be symbolized by

$$\text{cov}(n+1,\psi) = \sum_{k=n+1}^{\infty} \sigma_k^2 \, P_k(\cos\psi) \, . \tag{4.4a}$$

Here "cov" depicts the geoidal covariances, while "var" depicts the geoidal variances, both due to the neglected degrees (from n+1 to infinity). Since $P_k(1) \equiv 1$, one has

$$var(n+1) = \sum_{k=n+1}^{\infty} \sigma_k^2 \ . \tag{4.4b}$$

In practical computations the degree "∞" is substituted for by n_{max} which, as indicated earlier, can be replaced by 500 or 1,000, or some other sufficiently large number.

Appendix 1 features a computer program using the algorithm (4.4a,b), where the degree variances are given in (4.3) and the well-known recurrent relationship for the Legendre polynomials reads

$$P_k(z) = (1/k)[z(2k-1)P_{k-1}(z) - (k-1)P_{k-2}(z)] \ ,$$

starting with

$$P_0(z) = 1 \ , \qquad P_1(z) = z \ .$$

This formula is contained in the subroutine "Legen" also listed.

The symbols utilized by the program in Appendix 1 are:

NPROB ... number of different problems to be treated,

and within each problem:

IORDER ... n_{max} (dimensioned for 1,000),

NPSI ... number of different angles "ψ" (dimensioned for 30),

NN ... number of different truncations "n" (dimensioned for 20).

Following NPSI the input consists of the individual angles ψ in degrees, and following NN the input consists of the individual truncations n in the

-24-

descending order. In the computer run carried out for the present purpose
NPROB has been 1, IORDER has been 500, NPSI has been 27, the (27) values of
ψ have run from 0 to 13^0 in 0.5^0 intervals, NN has been 1, and the (one)
desired truncation has been n = 14. For comparison purposes, the values
associated with $\psi = 15^0$ and $\psi = 30^0$ will also be presented.

The values corresponding to the (14,14) truncated model as obtained with
the above computer program are (ψ is in ^{0}, covψ is in m^2; for $\psi=0$ "cov" means
"var"):

$$(4.5)$$

ψ :	0	0.5	1.0	1.5	2.0	2.5	3.0	3.5	4.0
covψ:	23.869	23.102	21.496	19.501	17.315	15.055	12.798	10.600	8.503

ψ :	4.5	5.0	5.5	6.0	6.5	7.0	7.5	8.0	8.5
covψ:	6.533	4.710	3.050	1.560	0.244	-0.897	-1.866	-2.667	-3.306

ψ :	9.0	9.5	10.0	10.5	11.0	11.5	12.0	12.5	13.0
covψ:	-3.792	-4.136	-4.347	-4.437	-4.418	-4.304	-4.105	-3.835	-3.507

The covariances whose magnitude is less than 1/3 of the variance ($23.869m^2$)
are deemed relatively unimportant for the adjustment. Thus the factor ρ
appearing in the modified matrix C in (4.1) will be computed using only the
first nine values (for ψ ranging from 0 to 4^0). The covariance values at
$\psi=4^0$ and $\psi=4.5^0$ correspond to 35% and 27% of the variance, respectively. The
covariance value at $\psi=13^0$ does not even attain 15% of the variance, and the
covariance magnitudes diminish quite rapidly beyond this angle. For example,
for $\psi=15^0$ the covariance value is -1.841 (under 8% of the variance) and for
$\psi=30^0$ this value is -0.574 (about 2% of the variance). The values of the
modified covariance function corresponding to (4.1) would approach zero even

faster. It thus appears to be amply sufficient to extend this analysis as far as $\psi=13^0$ and not beyond.

4.3 Estimated and Modified Variance-Covariances

As has been already indicated in [Blaha, 1982], the geoidal variance from (4.5) -- or, equivalently, its square root $\sigma = 4.886m$ -- appears to be conservative when compared to its estimate using SEASAT altimeter observations. The final root mean square (rms) of the constant terms of observation equations from all the SEASAT arcs in a (14,14) S.H. model has been computed as 3.6064m and designated as the estimate $\hat{\sigma}(total)$. The estimate of the variance $(\hat{\sigma}^2)$ due to the truncation is then found as

$$\hat{\sigma}^2 = \hat{\sigma}^2(total) - \hat{\sigma}^2(s.v.) - \hat{\sigma}^2(sea\ surf.) - \hat{\sigma}^2(altim.) - \hat{\sigma}^2(S.H.) - \hat{\sigma}^2(algor.),$$

where $\hat{\sigma}(s.v.)$ is the estimated sigma due to the s.v. parameters, in particular, due to the uncertainty in the "up" component of the precise ephemeris used and given a priori as 1.6m; $\hat{\sigma}(sea\ surf.)$ is the estimated sigma due to the tides and other sea surface effects, assumed to be in the vicinity of 0.3m; $\hat{\sigma}(altim.)$ is the estimated sigma of the altimeter noise, assumed to be 0.2m; $\hat{\sigma}(S.H.)$ is the estimated sigma due to the errors in the a priori values of the (14,14) set of S.H. potential coefficients used, whose value is unknown but considered small and adopted as zero; and $\hat{\sigma}(algor.)$ is the estimated sigma due to the short-arc algorithm, also considered small and adopted as zero.

With the above values one finds

$$\hat{\sigma}^2 = 10.3161m^2 ,\tag{4.6}$$

which is substantially smaller than

$$\sigma^2 = 23.869m^2 ,\tag{4.7}$$

as given in (4.5). From (4.6) one has $\hat{\sigma} = 3.212$m, which may still be slightly conservative due especially to the assumption $\hat{\sigma}(\text{S.H.}) = 0$. In any event, the effect of $\hat{\sigma}(\text{s.v.})$ represents the largest reduction of $\hat{\sigma}(\text{total})$; with only these two quantities present the value of $\hat{\sigma}$ would have been 3.232m, differing little from 3.212m computed above.

Due to the lack of other indications, we assume that the variance-covariances of (4.5) should be scaled down by the factor $\hat{\sigma}^2/\sigma^2$ computed from (4.6) and (4.7) in order to yield what will be called the estimated geoidal variance-covariances. This factor is

$$\hat{\sigma}^2/\sigma^2 = 0.4322. \tag{4.8}$$

The ratio $\hat{\sigma}/\sigma$ is 0.657, or the estimated sigma is about 2/3 of the theoretical sigma. In applying the factor in (4.8) to (4.5) one obtains (4.9) below where, however, the estimated variance of 10.3161m^2 has been increased by $(0.4\text{m})^2$. This increase is due to the altimeter noise represented by the variance $(0.2\text{m})^2$, as well as to other modeled and unmodeled effects. The sigma corresponding to this final variance is 3.237m. The resulting estimates are

(4.9)

ψ :	0	0.5	1.0	1.5	2.0	2.5	3.0	3.5	4.0
covψ:	10.476	9.985	9.291	8.428	7.484	6.507	5.531	4.581	3.675

ψ :	4.5	5.0	5.5	6.0	6.5	7.0	7.5	8.0	8.5
covψ:	2.824	2.036	1.318	0.674	0.105	-0.388	-0.806	-1.153	-1.429

ψ :	9.0	9.5	10.0	10.5	11.0	11.5	12.0	12.5	13.0
covψ:	-1.639	-1.788	-1.879	-1.918	-1.909	-1.860	-1.774	-1.657	-1.516

As indicated earlier, only the values between $\psi=0$ and $\psi=4°$ will be used in computing the modified variance-covariances from the estimated variance-covariances of (4.9). In particular, a coefficient ρ is sought which gives a covariance in (4.9) upon the multiplication by the preceding value. The eight successive ratios obtained from the first nine consecutive values in (4.9) are

0.9531, 0.9305, 0.9071, 0.8880, 0.8695, 0.8500, 0.8282, 0.8022.

Beyond $4°$ the ratios would decrease more rapidly (0.7684, 0.7210, 0.6473, etc). The average coefficient computed from the above eight values, and its second power, are

$$\rho = 0.8786 , \qquad \rho^2 = 0.7719 . \qquad\qquad (4.10a,b)$$

Upon applying (4.10a) to 10.476 in (4.9), the modified covariances are, in succession,

(4.11)

ψ :	0	0.5	1.0	1.5	2.0	2.5	3.0	3.5	4.0
covψ:	10.476	9.204	8.087	7.105	6.243	5.485	4.819	4.234	3.720

ψ :	4.5	5.0	5.5	6.0	6.5	7.0	7.5	8.0	8.5
covψ:	3.268	2.871	2.523	2.217	1.948	1.711	1.503	1.321	1.161

ψ :	9.0	9.5	10.0	10.5	11.0	11.5	12.0	12.5	13.0
covψ:	1.020	0.896	0.787	0.692	0.608	0.534	0.469	0.412	0.362

4.4 Least-Squares Adjustment Using Three Types of Variance-Covariances

At this point three weighting schemes for observational intervals of $0.5°$, sufficient for a $1°$- or a $2°$-geoidal resolution, are presented. The first, "rigorous" case is characterized by the C matrix of dimensions $(m \times m)$, where m is now taken as 27, whose entries correspond to the estimated variance-covariances of (4.9):

$$C_1 = \begin{bmatrix} 10.476 & 9.985 & 9.291 & \cdots & -1.657 & -1.516 \\ 9.985 & 10.476 & 9.985 & \cdots & -1.774 & -1.657 \\ 9.291 & 9.985 & 10.476 & \cdots & -1.860 & -1.774 \\ \vdots & & & & & \\ -1.516 & -1.657 & -1.774 & \cdots & 9.985 & 10.476 \end{bmatrix}.$$

The inversion of this matrix yields a fully populated P_1 matrix.

The second, tri-diagonal case is characterized by the C matrix of dimensions $(m \times m)$, where again $m = 27$, whose entries correspond to the modified variance-covariances of (4.11), namely

$$C_2 = \begin{bmatrix} 10.476 & 9.204 & 8.087 & \cdots & 0.412 & 0.362 \\ 9.204 & 10.476 & 9.204 & \cdots & 0.469 & 0.412 \\ 8.087 & 9.204 & 10.476 & \cdots & 0.534 & 0.469 \\ \vdots & & & & & \\ 0.362 & 0.412 & 0.469 & \cdots & 9.204 & 10.476 \end{bmatrix}.$$

The tri-diagonal weight matrix is given as in (4.2), where the value "σ^2" is 10.476 and ρ, ρ^2 are given in (4.10a,b). The result is

$$P_2 = \begin{bmatrix} a & b & 0 & 0 & 0 & \ldots & 0 & 0 \\ b & c & b & 0 & 0 & \ldots & 0 & 0 \\ 0 & b & c & b & 0 & \ldots & 0 & 0 \\ \vdots & & & & & & & \\ 0 & 0 & 0 & \ldots\ldots\ldots\ldots & b & a \end{bmatrix} , \tag{4.12}$$

with

$$a = 0.4185, \qquad b = -0.3677, \qquad c = 0.7415 . \tag{4.13}$$

The third, diagonal case is characterized by the simplification in which all the covariances are ignored, resulting in the following matrices:

$$C_3 = 10.476 \; I ,$$

$$P_3 = 0.09546 \; I , \tag{4.14}$$

where I is the identity matrix of dimensions ($m \times m$), again with $m = 27$.

In the first case, the formation of normal equations for one arc containing m observations (on SEASAT arcs $m \leq 54$) proceeds without any simplification according to the standard formula

$$(A^T P_1 A)x = A^T P_1 \epsilon , \tag{4.15}$$

-31-

where A, consisting of the rows A_i, $i = 1, 2, \ldots m$, is the (design) matrix of observation equations and ε is the vector containing m constant terms (ε_i), x being the vector of parameters. Here all the m rows of A have to be retained in the computer core as has already been indicated. The same holds true for the m constant terms.

In the second case, the matrix of normal equations, $A^T P_2 A$, is formulated in a much simpler manner, namely

$$A^T P_2 A = (aA_1^T + bA_2^T)A_1 + \sum_{i=2}^{m-1} [cA_i^T + b(A_{i-1}^T + A_{i+1}^T)]A_i + (aA_m^T + bA_{m-1}^T)A_m . \quad (4.16)$$

The right-hand side of normal equations, $A^T P_2 \varepsilon$, is computed as above, except that each symbol A_k, $k = 1, 2, \ldots m$, is replaced by the corresponding ε_k. The middle terms on the right-hand side of (4.16) indicate that only three rows of A and the corresponding three elements of ε are needed in the computer core at any one time. Clearly, the number of scalar multiplications in this process is greatly reduced when compared to the first case.

The third case is the simplest, where

$$A^T P_3 A = 0.09546 \sum_{i=1}^{m} A_i^T A_i . \quad (4.17)$$

The computation of $A^T P_3 \varepsilon$ proceeds as above except that each symbol A_i is to be replaced by the corresponding ε_i. Here only one row of A and the corresponding element of ε are needed in the computer core at any one time. The number of scalar multiplications is lower than in the previous case, but the difference is not great. In fact, the decrease is approximately equal to the (2/u)-multiple of the total number of scalar multiplications, where u is the number of parameters.

Although the second case is about as economical as the third case, its results are likely to be much closer to the "rigorous" (first) case than the results of the third case. At first sight, this can be assessed as follows. Let the differences between the second and first cases be called the second case errors. Upon comparing the values in (4.11) with those in (4.9), these errors (between $\psi=0$ and $\psi=13°$) are

(4.18)

0, -0.781, -1.204, -1.323, -1.241, -1.022, -0.712, -0.347, 0.045,

0.444, 0.835, 1.205, 1.543, 1.843, 2.099, 2.309, 2.474, 2.590,

2.659, 2.684, 2.666, 2.610, 2.517, 2.394, 2.243, 2.069, 1.878.

For $15°$ and $30°$ these values would be 1.012 and 0.252, respectively. The rms of these errors up to $\psi=4°$ is $0.937m^2$, while the total rms including all the values in (4.18) is $1.869m^2$.

Similar to the above, the differences between the third and first cases, called the third case errors, are obtained directly from (4.9) as

(4.19)

0, -9.985, -9.291, -8.428, -7.484, -6.507, -5.531, -4.581, -3.675,

-2.824, -2.036, -1.318, -0.674, -0.105, 0.388, 0.806, 1.153, 1.429,

1.639, 1.788, 1.879, 1.918, 1.909, 1.860, 1.774, 1.657, 1.516.

For $15°$ and $30°$ these values would be 0.796 and 0.248, respectively. The rms of these errors up to $\psi=4°$ is $7.250m^2$, while the total rms including all the values in (4.19) is $4.240m^2$. It is thus apparent that the second case is far superior to the third case with regard to accuracy, the first case representing the standard of comparison. In particular, the rms of the second case errors

attains only about 44% of the rms of the third case errors. The comparison

of the solutions in a specific example that follows will confirm the superior

quality of the second case (versus the third case) from yet another angle.

4.5 Practical Example

In this example only $m=13$ geoid undulations considered as observations are used, distributed in $1°$ intervals and spanning a $12°$-arc. Upon taking every other entry of (4.9) into account, the first case is now represented by

$$C_1 = \begin{bmatrix} 10.476 & 9.291 & 7.484 \ldots & -1.909 & -1.774 \\ 9.291 & 10.476 & 9.291 \ldots & -1.879 & -1.909 \\ 7.484 & 9.291 & 10.476 \ldots & -1.639 & -1.879 \\ \vdots & & & & \\ -1.774 & -1.909 & -1.879 \ldots & 9.291 & 10.476 \end{bmatrix}. \qquad (4.20)$$

In the second case, every other entry of (4.11) similarly entails

$$C_2 = \begin{bmatrix} 10.476 & 8.087 & 6.243 \ldots & 0.608 & 0.469 \\ 8.087 & 10.476 & 8.087 \ldots & 0.787 & 0.608 \\ 6.243 & 8.087 & 10.476 \ldots & 1.020 & 0.787 \\ \vdots & & & & \\ 0.469 & 0.608 & 0.787 \ldots & 8.087 & 10.476 \end{bmatrix}.$$

The new ρ is now 0.7719 (i.e., ρ^2 from 4.10b) and the new ρ^2 is 0.5958. In analogy to the procedure that yielded (4.12) and (4.13) one obtains

$$(4.21)$$

$$P_2 = \begin{bmatrix} 0.2362 & -0.1823 & 0 & 0 & \ldots\ldots & 0 & 0 \\ -0.1823 & 0.3769 & -0.1823 & 0 & \ldots\ldots & 0 & 0 \\ 0 & -0.1823 & 0.3769 & -0.1823 & \ldots\ldots & 0 & 0 \\ \vdots & & & & & & \\ 0 & 0 & 0 & \ldots\ldots\ldots\ldots\ldots & -0.1823 & 0.2362 \end{bmatrix} .$$

Finally, the form of the C and P matrices in the third case is

$$C_3 = 10.476 \ I \ ,$$

$$P_3 = 0.09546 \ I \ , \tag{4.22}$$

which corresponds to (4.14) and the equation that preceded it, except that now $m = 13$.

The 13 observations considered are used to adjust one parameter, taken as a point-mass magnitude. The point mass itself is chosen to have a central location with respect to the arc, and to be located at the depth $d = 1,144$ km underneath the earth's surface represented by a sphere of radius $R = 6,371$ km. Thus the central angle ψ varies between 0 and 6° on either side of the point mass. The mathematical model for geoid undulations can now be written as

$$N_i = (1/G)(kM)_j / \ell_{ij} \ , \qquad i = 1,2, \ldots m \ , \tag{4.23}$$

where G is the average value of gravity adopted as 980 gal; $(kM)_j \equiv x$ is the

-36-

unknown parameter, i.e., the gravitational constant times the mass of the point mass "j"; and ℓ_{ij} is the distance between the observational point "i" and the point mass "j". The latter is computed as

$$\ell_{ij} = \{[(R-d)\sin\psi_{ij}]^2 + [R-(R-d)\cos\psi_{ij}]^2\}^{1/2} , \qquad (4.24)$$

where ψ_{ij} is the angle ψ corresponding to the above points i and j.

The 13 observations of geoid undulations (in meters) are simulated in a symmetrical manner, the first and the last being zero and the middle one directly above the point mass being 3.5m, as follows:

$$0.000, \quad 0.906, \quad 1.750, \quad 2.475, \quad 3.031, \quad 3.381, \quad 3.500,$$
$$3.381, \quad 3.031, \quad 2.475, \quad 1.750, \quad 0.906, \quad 0.000. \qquad (4.25)$$

These values represent the elements of the vector ϵ encountered earlier. The units are chosen such that x is expressed in terms of 10^{-6} times the earth's kM (the latter is $3.986005 \times 10^{14} m^3/sec^2$). The matrix A has now the dimensions (1×13); the values in this row, symmetric about its middle element, are

$$31.440, \quad 32.542, \quad 33.536, \quad 34.375, \quad 35.015, \quad 35.417, \quad 35.554,$$
$$35.417, \quad 35.015, \quad 34.375, \quad 33.536, \quad 32.542, \quad 31.440.$$
$$(4.26)$$

Similar to (4.15), the least-squares adjustment yields

$$\hat{x} = (A^TPA)^{-1}A^TP\epsilon , \qquad (4.27a)$$

$$\sigma_{\hat{x}}^2 = (A^TPA)^{-1} , \qquad (4.27b)$$

which entails three cases, $P=P_1$, $P=P_2$ and $P=P_3$, in agreement with the previous

-37-

classifications. In terms of the transformation $x' = 100x$ (x' is thus expressed in 10^{-8} of the earth's kM), the pertinent results can be grouped in Table 1, which is self-explanatory. This table shows the error in the tri-diagonal solution as being only 39% of the error in the diagonal solution. The error in the sigma of the tri-diagonal solution is even smaller, amounting to merely 22% of the error in the sigma of the diagonal solution. Although this example is quite specialized, it nevertheless illustrates that the tri-diagonal set-up is likely to match the rigorous setup much more closely than would be possible with the diagonal setup.

Case	Name	$\hat{x}'$	Error	$\sigma_{\hat{x}'}$	Error
1	"rigor."	3.675	--	5.491	--
2	tri-diag.	4.651	+0.976	6.121	+0.630
3	diagonal	6.179	+2.504	2.649	-2.842

Table 1

The least-squares solution and its sigma, together with their errors, in the three weighting schemes considered; the first case is taken as an errorless standard.

5. LARGE AREA ADJUSTMENT WITH POINT-MASS AND TIDAL PARAMETERS BASED ON THE BANDED-BORDERED STRUCTURE OF NORMAL EQUATIONS

5.1 General Discussion

This chapter is a natural continuation of Chapter 3 in [Blaha, 1983], where a large area adjustment algorithm was developed in terms of point-mass (P.M.) magnitudes as parameters. That algorithm was characterized by a banded structure of normal equations. It was based on a first-phase global adjustment of satellite altimetry which, optionally, could have included also certain tidal parameters. In the next section the above algorithm will be extended, in the sense that selected tidal parameters will optionally be subject to (re)adjustment also in the second-phase adjustment of satellite altimetry based on point masses.

Since the only modification of the previous P.M. algorithm consists in adding the parameters expressing certain temporal variations in the ocean surface, the considerations of the underlying gravity field of the earth are unchanged from the previous AFGL report ([Blaha, 1983]) to the present one. It may then be useful to review this approach as it relates to the gravity field, and compare it with the P.M. approach developed in recent years and described in the paper [Kautzleben and Barthelmes, 1983]. The former will be called "our approach" while the latter will be abbreviated as [KB] in the forthcoming comparisons.

In our approach, the global gravity field of the earth is split into the field "A", called the global normal field, and the field "B", called the anomalistic field. The field A is not an ellipsoidal field, but a field

represented by a (14,14) spherical-harmonic expansion of the earth's potential; all the anomalistic geophysical quantities, such as geoid undulations, gravity anomalies, deflections of the vertical, etc., refer to this field. The field B is described by an equilateral grid of point masses at a certain depth underneath the spherical surface approximating the earth's surface (due to the relatively high resolution power of the field A as compared to the ellipsoidal field, the spherical approximation is acceptable).

In the [KB] approach the gravity field is similarly split as can be gathered, e.g., from the statement on page 308:

"... the anomalies refer to a global normal field given by a spherical harmonic analysis up to the fourth order inclusively. Splitting up the gravity field in a normal field and the field of anomalies is a mathematically exact procedure."

The basic difference between the two approaches stems merely from the fourteenth order spherical-harmonic expansion characteristic of our approach contrasted to the fourth order expansion of [KB]. This difference is more of a practical than conceptual nature.

Initially, [KB] addressed the problem where not only the P.M. magnitudes were subject to a least-squares adjustment, but also their positions. Furthermore, their number was not fixed. In our approach the number of point masses as well as their locations are decided upon beforehand; according to the above definition they are distributed in an equilateral grid. However, [KB] comes closer to our approach through the text on page 310:

"There is a way known [that] uses only points which are distributed equidistantly on the surface of a sphere in the Earth's interior and where the problem is reduced to determine the best radius of that sphere and [the magnitudes] of the masses of the points mentioned."

-40-

It thus follows that in addition to the solution of P.M. magnitudes as in our approach, [KB] also determines one additional parameter, the depth of these masses. The common feature of both approaches is the same depth of all the point masses present in the adjustment.

The fixed depth of point masses in our approach implies that the entire adjustment model is linear in the parameters. This allows us to adopt zero starting values for the parameters -- which are unknown a priori -- without the need for an iterated solution. On the other hand, as it transpires from [KB] the depth (or radius) of the point masses is a non-linear parameter. Therefore, its good starting value should be known a priori in order to avoid iterations in the adjustment and/or avoid the solution converging to a false minimum. Clearly, one could perform preliminary tests using different values of the depth parameter and find the most suitable starting value for the full scale adjustment. But this can again be related to our approach, where different depths of point masses can be entered into adjustment runs carried out over one and the same limited area. The depth resulting in the best fit can then be adopted for the desired full scale adjustment. Accordingly, whether or not the one additional parameter, the depth of the point masses, should also be subject to adjustment is essentially a practical matter.

A variation of the P.M. approach addressed in [KB] is well worth mentioning. It is based on successive solutions of point masses, starting with two of them, as is described on page 310:

"After both of these point masses have been determined their field is subtracted from all the measured values. Based on the new distribution of the measured values analogously the coordinates and the masses of the next two point masses are calculated. This algorithm can be continued up to any number of point masses."

It is clear that whether two or more than two point masses are treated at a time in this manner is an arbitrary decision. One could as well consider all of the point masses and subtract their field from the measured values in one step. This is, in fact, the principle used in our approach, i.e., a simultaneous least-squares adjustment of all the P.M. parameters.

Our simultaneous approach could have, indeed, some practical drawbacks from the computer-core and run-time standpoints. However, the development of a banded (or banded-bordered) structure of normal equations can bridge these difficulties. Such a structure results in a ten-fold increase in efficiency, and has allowed the increase in the number of P.M. parameters adjusted simultaneously from about 200 to 2,000.

One of the three basic steps leading to the banded structure of normal equations described in Chapter 3 of [Blaha, 1983] resides in neglecting a point mass when forming the observation equation for a given observation if this mass is farther from the observation point than a predetermined limit. But this is compatible with the procedure used in [KB] on page 310:

> "To determine the improved values for the coordinates and for the masses of both these point masses by the procedure described above not all the measured values at the whole surface of the Earth but only values in the neighbourhood of these point masses are used."

The approximation of neglecting an observation when its influence on a point mass is only a fraction of the maximum influence (for an observation directly above the point mass) is well worth making, both in [KB] and in our approach. One can thus conclude that although some of their individual features may differ, the two approaches on the whole are conceptually quite similar.

5.2 Banded-Bordered Algorithm

The task addressed in this section is the extension of the concept and the algorithm for large-scale adjustments of satellite altimetry using point masses. Whereas in Chapter 3 of [Blaha, 1983] special attention was paid to the P.M. algorithm applicable to a banded system of normal equations eventually resolved by the "modified Choleski algorithm", the present extension concerns a banded-bordered system of normal equations. It will become apparent that the former system is a special case of the latter.

First, the highlights of the resolution of the banded system are re-capitulated. The observation equations in usual notations read

$$V = AX - (L^b - L^o) , \qquad (5.1)$$

where

A = (design) matrix of observation equations,

X = vector of parameters (here the P.M. magnitudes),

$-(L^b - L^o)$ = vector of constant terms of observation equations,

and where

L^b = observed values of the observables,

L^o = initial values of the observables.

The normal equations for the above system are

$$NX = U , \tag{5.2}$$

where

$$N = A^T A , \qquad U = A^T(L^b - L^\circ) . \tag{5.3a,b}$$

The weight matrix of the observations, P, is not considered here because the matrix A is scaled; at this point one would simply have P=I (a unit matrix). In the case of independent observations the scaling is accomplished by dividing each observation equation by the appropriate sigma, which was used in [Blaha, 1983] and mentioned on page 33 therein. In the situation with weighted parameters the appropriate weight matrix P_x would be added to the matrix of normal equations, N. However, the initial values of the P.M. parameters (taken as zeros) are not attributed any weight.

The solution of normal equations and the variance-covariance matrix of the parameters are expressed by

$$X = N^{-1}U , \qquad \Sigma_X = N^{-1} . \tag{5.4a,b}$$

With regard to a w-vector of linear combinations of parameters, we have

$$F = \overline{U}^T X , \qquad \Sigma_F = \overline{U}^T N^{-1} \overline{U} , \tag{5.5a,b}$$

where $\overline{U}$ is a matrix of dimensions (n×w), n being the number of parameters. The variance-covariance matrix of the parameters is obtained by substituting I for $\overline{U}$ in (5.5b), which is the procedure adopted in the modified Choleski algorithm.

As is explained on page 37 of [Blaha, 1983], the triangular decomposition of the positive-definite matrix N amounts to writing

$$T^TT = N , \qquad N^{-1} = T^{-1}(T^T)^{-1} ; \qquad (5.6a,b)$$

$$T^TR = U , \qquad R = (T^T)^{-1}U ; \qquad (5.7a,b)$$

$$T^T\overline{R} = \overline{U} , \qquad \overline{R} = (T^T)^{-1}\overline{U} . \qquad (5.8a,b)$$

The matrix T of dimensions (n×n) is computed according to the explanation given on pages 38 and 39 of the above reference, listing also the remaining part of the algorithm ("regular" Choleski algorithm at this point) for the elements of R, $\overline{R}$ and X. The latter is computed via the "back substitution", *corresponding to*

$$TX = R , \qquad X = T^{-1}R , \qquad (5.9a,b)$$

where (5.9a) is the consequence of (5.2) being pre-multiplied by $(T^T)^{-1}$, and (5.9b) follows either from (5.9a) or from (5.4a) with (5.6b), (5.7a). Finally, (5.5b) can be expressed as

$$\Sigma_F = \overline{R}^T\overline{R} , \qquad (5.10)$$

which leads to Σ_X upon substituting I for $\overline{U}$.

In the present task, the vector A'X' is added to the right-hand side of (5.1), subject to the same least-squares process. Here X' represents the "overcorrections" to the tidal parameters which were involved in the first-phase global altimeter adjustment together with the spherical-harmonic poten-tial coefficients and the state vector parameters; the matrix A' of the

partial derivatives with respect to the tidal parameters is adopted from that adjustment (its elements are stored on a tape for each altimeter observation). The initial values for X' are set to zero and the weight matrix for X', denoted $P_{X'}$, reflects the reliability of the previous solution for the tidal parameters, i.e., the strength of the zero initial values. The extended observation equations read

$$V = \begin{bmatrix} A & A' \end{bmatrix} \begin{bmatrix} X \\ X' \end{bmatrix} - (L^b - L^o) \ . \tag{5.11}$$

The extended normal equations then are

$$\begin{bmatrix} N & \overline{\overline{U}} \\ \overline{\overline{U}}^T & N' \end{bmatrix} \begin{bmatrix} X \\ X' \end{bmatrix} = \begin{bmatrix} U \\ U' \end{bmatrix} \ , \tag{5.12}$$

with the new notations,

$$\overline{\overline{U}} = A^T A' \ , \qquad N' = A'^T A' + P_{X'} \ , \qquad U' = A'^T (L^b - L^o) \ . \tag{5.13a,b,c}$$

The weight matrix P is incorporated in A' through the same scaling as before.

The solution of the above normal equations and the variance-covariance matrix of the parameters are given, respectively, as

$$\begin{bmatrix} X \\ X' \end{bmatrix} = \begin{bmatrix} N & \overline{\overline{U}} \\ \overline{\overline{U}}^T & N' \end{bmatrix}^{-1} \begin{bmatrix} U \\ U' \end{bmatrix} \ , \qquad \Sigma_{\substack{X \\ X'}} = \begin{bmatrix} N & \overline{\overline{U}} \\ \overline{\overline{U}}^T & N' \end{bmatrix}^{-1} \ . \tag{5.14a,b}$$

Upon using equation (11a) from [Blaha, 1976], one has

$$\begin{bmatrix} N & \overline{\overline{U}} \\ \overline{\overline{U}}^T & N' \end{bmatrix}^{-1} = \begin{bmatrix} N^{-1} + N^{-1}\overline{\overline{U}}H\overline{\overline{U}}^TN^{-1} & -N^{-1}\overline{\overline{U}}H \\ -H\overline{\overline{U}}^TN^{-1} & H \end{bmatrix} \tag{5.15}$$

where

$$H = (N' - \overline{\overline{U}}^TN^{-1}\overline{\overline{U}})^{-1} . \tag{5.16}$$

With (5.15) and (5.16), equations (5.14a,b) lead to

$$X' = (N' - \overline{\overline{U}}^TN^{-1}\overline{\overline{U}})^{-1}(U' - \overline{\overline{U}}^TN^{-1}U) , \tag{5.17a}$$

$$X = N^{-1}(U - \overline{\overline{U}}X') ; \tag{5.17b}$$

$$\Sigma_{X'} = (N' - \overline{\overline{U}}^TN^{-1}\overline{\overline{U}})^{-1} , \tag{5.18a}$$

$$\Sigma_X = N^{-1} + N^{-1}\overline{\overline{U}}(N' - \overline{\overline{U}}^TN^{-1}\overline{\overline{U}})^{-1}\overline{\overline{U}}^TN^{-1} . \tag{5.18b}$$

In analogy to (5.5a,b), we write for linear functions of X' and X, respectively:

$$F' = \overline{\overline{U}}'^T X' , \qquad \Sigma_{F'} = \overline{\overline{U}}'^T \Sigma_{X'}\overline{\overline{U}}' , \tag{5.19a,b}$$

$$F = \overline{U}^T X , \qquad \Sigma_F = \overline{U}^T \Sigma_X \overline{U} , \tag{5.20a,b}$$

where the vector F' has w' elements and $\overline{\overline{U}}'$ is a matrix of dimensions (n'×w'), n' being the number of tidal parameters (i.e., the number of elements in X').

The variance-covariance matrices for X' and X are obtained upon setting $\overline{\overline{U}}'=I$ in (5.19b) and $\overline{U}=I$ in (5.20b), respectively.

As an extension of (5.7a,b) and (5.8a,b), new notations are introduced, namely

$$T^T\overline{\overline{R}} = \overline{\overline{U}} \,, \qquad \overline{\overline{R}} = (T^T)^{-1}\overline{\overline{U}} \,. \tag{5.21a,b}$$

Thus the following equivalent expressions are obtained:

$$\overline{\overline{U}}^T N^{-1}\overline{\overline{U}} = \overline{\overline{R}}^T\overline{\overline{R}} \,, \qquad \overline{\overline{U}}^T N^{-1} U = \overline{\overline{R}}^T R \,, \qquad N^{-1}\overline{\overline{U}} = T^{-1}\overline{\overline{R}} \,.$$

Accordingly, (5.17a,b),(5.19b) and (5.20b) are rewritten as

$$X' = (N' - \overline{\overline{R}}^T\overline{\overline{R}})^{-1}(U' - \overline{\overline{R}}^T R) \,, \tag{5.22a}$$

$$X = T^{-1}(R - \overline{\overline{R}}X') \,; \tag{5.22b}$$

$$\Sigma_{F'} = \overline{\overline{U}}'^{\,T}(N' - \overline{\overline{R}}^T\overline{\overline{R}})^{-1}\overline{\overline{U}}' \,, \tag{5.23a}$$

$$\Sigma_F = \overline{R}^T\overline{R} + \overline{\overline{R}}^T\overline{\overline{R}}(N' - \overline{\overline{R}}^T\overline{\overline{R}})^{-1}\overline{\overline{R}}^T\overline{\overline{R}} \,, \tag{5.23b}$$

where, in addition to (5.21b), also the previous notations (5.6b) and (5.8b) have been used.

Since H in (5.15) and thus also $H^{-1}=N'-\overline{\overline{R}}^T\overline{\overline{R}}$ are positive-definite matrices, one can express X' in (5.22a) and $\Sigma_{F'}$ in (5.23a) in a complete analogy to the process represented by the steps (5.6a)-(5.10). In particular, we write

$$T'^T T' = N' - \overline{\overline{R}}^T\overline{\overline{R}} \,, \qquad (N' - \overline{\overline{R}}^T\overline{\overline{R}})^{-1} = T'^{-1}(T'^T)^{-1} \,; \tag{5.24a,b}$$

$$T'^T R' = U' - \overline{\overline{R}}^T R \,, \qquad R' = (T'^T)^{-1}(U' - \overline{\overline{R}}^T R) \,; \tag{5.25a,b}$$

$$T'^T\overline{\overline{R}}' = \overline{\overline{U}}' \,, \qquad \overline{\overline{R}}' = (T'^T)^{-1}\overline{\overline{U}}' \,. \tag{5.26a,b}$$

This then leads to

$$T'X' = R' , \qquad X' = T'^{-1}R' , \tag{5.27a,b}$$

$$\Sigma_{F'} = \overline{\overline{R}}'^{T}\overline{\overline{R}}' . \tag{5.28}$$

Upon adding one further notation, $\overline{R}'$, and using it in the relation

$$T'^{T}\overline{R}' = \overline{\overline{R}}^{T}\overline{R} , \qquad \overline{R}' = (T'^{T})^{-1}\overline{\overline{R}}^{T}\overline{R} , \tag{5.29a,b}$$

it follows from (5.23b) that

$$\Sigma_{F} = \overline{R}^{T}\overline{R} + \overline{R}'^{T}\overline{R}' . \tag{5.30}$$

The whole process can now be recapitulated in six steps as follows.

1) Equations (5.6a), (5.7a), (5.8a) and (5.21a) describe the part of
   the algorithm that can be schematically represented as

$$T^{T} \underset{ n\times n | n\times 1 | n\times w | \underline{n\times n'}}{[\, T \mid R \mid \overline{R} \mid \overline{\overline{R}} \,]} = \underset{ n\times n | n\times 1 | n\times w | \underline{n\times n'}}{[\, N \mid U \mid \overline{U} \mid \overline{\overline{U}} \,]} ,$$

where the dimensions are also indicated and where the matrices under-
lined by a dashed line pertain to the new, "border" part of the
algorithm. From here T, R, $\overline{R}$ and $\overline{\overline{R}}$ are all computed as in the process
mentioned following (5.8a,b).

2) Equations (5.24a), (5.25a), (5.29a) and (5.26a), respectively,
   describe the part

$$T'^{T} \underset{n'\times n' \,|\, n'\times 1 \,|\, n'\times w \,|\, n'\times w'}{[\, T' \mid R' \mid \overline{R}' \mid \overline{\overline{R}}' \,]} = \underset{n'\times n' \,|\, n'\times 1 \,|\, n'\times w \,|\, n'\times w'}{[\,(N'-\overline{\overline{R}}^{T}\overline{R}) \mid (U'-\overline{R}^{T}R) \mid \overline{\overline{R}}^{T}\overline{R} \mid \overline{\overline{U}}' \,]} ,$$

which pertains to the "border" part of the algorithm in its
entirety. From here T', R', $\bar{R}'$ and $\bar{\bar{R}}'$ are computed in the same
way as their unprimed counterparts above.

3) Equation (5.27a) is repeated as

$$\underbrace{T'}_{n' \times n'} \ \underbrace{X'}_{n' \times 1} = \underbrace{R'}_{n' \times 1} \ ,$$

which again pertains to the "border" part of the algorithm. It
yields X' upon the "back substitution".

4) Equation (5.22b) is rewritten as

$$\underbrace{T}_{n \times n} \ \underbrace{X}_{n \times 1} = (\ \underbrace{R}_{n \times 1} - \underbrace{\bar{\bar{R}} \ X'}_{n \times 1}\ ) \ ,$$

from which X is obtained by the "back substitution".

5) Equation (5.30) is rewritten as

$$\underbrace{\Sigma_F}_{w \times w} = \underbrace{\bar{R}^T \bar{R}}_{w \times w} + \underbrace{\bar{R}'^T \bar{R}'}_{w \times w} \ .$$

6) Finally, equation (5.28) is rewritten as

$$\underbrace{\Sigma_{F'}}_{w' \times w'} = \underbrace{\bar{\bar{R}}'^T \bar{\bar{R}}'}_{w' \times w'} \ .$$

All of the steps above must be carried out in the order indicated, except
perhaps for the steps 5) and 6). The banded system is seen as a special case
of the banded-bordered system above, the additions due to the "border" being
identified by the dashed lines. Thus the banded system as described in [Blaha,
1983] consists only of the steps 1), 4) and 5) with the self-evident simplifica-
tions. Advantage of the banded structure of normal equations -- in addition to

the advantage of N being positive-definite -- can be taken in the step 1) as described in the above reference, where N and T are compacted to form (b×n) matrices, b being the bandwidth; this reference uses the symbol $\tilde{T}$ for the modified matrix N while the symbol T is left unchanged.

The steps 1)-4) above are now depicted symbolically with regard to the replacements in the computer core as they are progressing in the course of the present "extended modified Choleski algorithm":

$$[\underset{b\times n}{\tilde{T}}]\;[\underset{n\times 1}{U}\;\vdots\;\underset{n\times w}{\bar{U}}\;\vdots\;\underset{\underline{n\times n'}}{\bar{\bar{U}}}\;]\;\rightarrow\;[\underset{b\times n}{T}]\;[\underset{n\times 1}{R}\;\vdots\;\underset{n\times w}{\bar{R}}\;\vdots\;\underset{\underline{n\times n'}}{\bar{\bar{R}}}\;],$$

$$[\underset{\underline{n'\times n'}}{N'-\bar{\bar{R}}^{T}\bar{\bar{R}}}\vdots\underset{n'\times 1}{U'-\bar{R}^{T}R}\vdots\underset{n'\times w}{\bar{R}^{T}\bar{R}}\vdots\underset{n'\times w'}{\bar{\bar{U}}'}\;]\rightarrow[\underset{n'\times n'}{T'}\;\vdots\;\underset{n'\times 1}{R'}\;\vdots\;\underset{n'\times w}{\bar{R}'}\;\vdots\;\underset{n'\times w'}{\bar{\bar{R}}'}\;]\;\rightarrow[\underset{n'\times n'}{T'}\;\vdots\;\underset{n'\times 1}{X'}\;\vdots\;\underset{n'\times w}{\bar{R}'}\;\vdots\;\underset{n'\times w'}{\bar{\bar{R}}'}\;],$$

$$[\underset{b\times n}{T}][\underset{n\times 1}{R-\bar{\bar{R}}X'}\;\vdots\;\underset{n\times w}{\bar{R}}\;\vdots\;\underset{\underline{n\times n'}}{\bar{\bar{R}}}\;]\rightarrow[\underset{b\times n}{T}][\underset{n\times 1}{X}\;\vdots\;\underset{n\times w}{\bar{R}}\;\vdots\;\underset{\underline{n\times n'}}{\bar{\bar{R}}}\;].$$

The steps 5) and 6) need not be listed again. This scheme provides for the resolution of the banded-bordered systems of normal equations. Here again, if the underlined parts are left out, one is in the presence of the algorithm for the banded systems as described in Chapter 3 of [Blaha, 1983].

6. LEAST-SQUARES COLLOCATION WITH NOISE AS A SECOND-PHASE ALTIMETRIC APPROACH

In Chapter 5 as well as in [Blaha, 1983] a second-phase geoidal
determination has been addressed via a "direct" approach, in the sense that
the observations subjected to the least-squares (L.S.) adjustment have
been treated at their original locations. The quotes are used to indicate
a special point of view, since in another aspect such an adjustment could
be considered as indirect. In particular, it proceeds to an evaluation of
the desired quantities describing the earth's gravity field (geoid undulations,
gravity anomalies, etc.) through intermediate quantities, namely the point
masses. Due to the simultaneous character of this adjustment with regard
to both the observations (minus the geoidal residuals at the original
locations) and the parameters (point-mass magnitudes), it is computationally
demanding. This is true especially for a large-scale adjustment, in which
case the area is subdivided into overlapping strips treated separately.

In attempts for an increasingly detailed representation of the earth's
gravity field on a global scale it thus becomes expedient to search for ways
which would complement the "direct" approach by using other methods than the
least-squares. For example, one could take advantage of integral formulas
and compute spherical-harmonic (S.H.) potential cofficients consistent with
the desired smoothing effect without proceeding to a simultaneous L.S.
adjustment of observations. The final result would be a uniform representa-
tion of the geoid and the earth's gravity field obtained for the whole globe
in a continuous, one-piece fashion. The trade-off would be the necessity
of using some kind of a "translocation" approach.

Various interpolation and approximation techniques exist where, unlike in the point-mass approach, the original observations are translocated to some strategically advantageous positions. When used in the role of interpolating the (residual) geoid undulations of satellite altimetry, the L.S. collocation with noise pioneered by Moritz [1980] could be considered as belonging to a "translocation" category. A global approach based on Moritz's collocation will constitute the main topic of this chapter. Besides serving in its own right, the collocation approach could be further exploited and result in a set of S.H. potential coefficients as suggested in the preceding paragraph.

The basic observed quantities to be used in the collocation approach are described in [Blaha, 1983]. They consist of the "observed" geoid undulations or, equivalently, of the corresponding high-resolution residuals which encompass the improvements due to the orbital and tidal adjustment of satellite altimetry. Just as the "direct" approach, the collocation approach and, eventually, the S.H. approach can also serve in predicting other geophysical quantities in addition to geoid undulations, such as gravity anomalies, deflections of the vertical, etc. Clearly, the S.H. approach would have to be carried out on a global scale. In all cases the final product is represented by geoidal contour maps and, optionally, by contour maps of other geophysical quantities, especially the gravity anomalies. And in all cases, the contour maps are desired on a global oceanic scale.

6.1 Simple Translocation Approach

This section is conceived as an illustration of a translocation approach which is the simplest but also the least accurate. In this approach, the location of an observation point is changed but the value of the "observed" geoid undulation is not modified in any way. A grid is generated by filling it with undulation values, each adopted simply as the value at the nearest observation point. The formation of a regional or global grid of geoid undulations is thus accomplished very fast, from which a contour map can be constructed by simple means such as polynomial interpolation (linear or higher-degree). In considering the distribution of SEASAT passes, one could generate an equilateral grid of dimensions $1^0 \times 1^0$ or larger. In order to facilitate the interpolation procedure in some practical cases, a geo-graphical grid may be generated instead.

The disadvantages of this approach are listed as

a) The values associated with the "observed" geoid could be grossly in error at the grid points.

b) Such errors are unpredictable, neither minimized nor estimable, due to the grid values obtained without any regard to statistical methodology.

c) The contours may contain additional errors due to the inter-polation procedure (a polynomial interpolation makes no provision for the physical characteristics of the quantity being inter-polated); in particular, the grid cannot be densified through a physically meaningful model before the application of the polynomial interpolation.

d) Contour maps of other geophysically meaningful quantities (e.g. gravity anomalies) cannot be constructed.

e) The geographical grid, if used, leads to an apparent increase in resolution at higher latitudes and in the E-W direction, which is completely artificial and in contradiction with the physical reality (the geoidal detail is independent of latitude or azimuth).

f) A great majority of observations are ignored.

6.2 Review of the Best Linear Prediction Algorithm

The approach just discussed can serve only for comparison purposes and does not represent the final outcome of satellite altimetry in any way. A meaningful outcome based on altimeter measurements can be obtained with the aid of the L.S. collocation with noise, to be described in the next sections. It will then become apparent that the shortcomings listed above as a) through f) disappear. However, before presenting this method we review its special case, called here the best linear prediction method, whose detailed derivation can be found in Appendix 2. In [Moritz, 1980] this case is called the error-less collocation.

In the context of satellite altimetry only one prediction may be performed at a time. Although the next section will present the algorithm for the L.S. collocation with noise in the matrix form, a "transliteration" similar to the one below would be exceedingly simple to carry out. In denoting the prediction point by J, and the observation points (where the geoid undulations are available) by 1, 2, ..., n, the following formulas in the best linear prediction approach can be transcribed from Appendix 2:

$$\hat{N}_J = M^T W , \tag{6.1}$$

where

$$M^T = \begin{bmatrix} D_{J1} & D_{J2} & \cdots & D_{Jn} \end{bmatrix} , \tag{6.2}$$

$$W = H^{-1} F , \tag{6.3}$$

with

$$H = \begin{bmatrix} D_o & D_{12} & \cdots & D_{1n} \\ & D_o & \cdots & D_{2n} \\ & & & \vdots \\ \text{symm.} & & & \\ & & & D_o \end{bmatrix} , \qquad (6.4)$$

$$F = \begin{bmatrix} N_1 & N_2 & \cdots & N_n \end{bmatrix}^T . \qquad (6.5)$$

In these formulas $D_o \equiv D(0)$, $D_{ij} \equiv D(\psi_{ij})$ are the values of the covariance function for geoid undulations, N_1, N_2, ..., N_n are the geoid undulations at the observation points, and $\hat{N}_J$ is the desired prediction of geoid undulation. The dispersion measure (v_N^2) due exclusively to the error of prediction is computed in this case as

$$v_N^2 = D_o - M^T H^{-1} M ,$$

and it can be viewed in a loose analogy to the variance in stochastic processes; in Appendix 2 it is a diagonal element of the dispersion matrix $M\{\varepsilon\varepsilon^T\}$.

If gravity anomalies are the predicted quantities (based on geoid undulations at the observation points), one can write formulas similar to those above:

$$\Delta\hat{g}_J = \tilde{M}^T W , \qquad (6.6)$$

where

$$\tilde{M}^T = \begin{bmatrix} H_{J1} & H_{J2} & \cdots & H_{Jn} \end{bmatrix} , \qquad (6.7)$$

-57-

and where W is the same vector as before, while $H_{ij} \equiv H(\psi_{ij})$ is the cross-covariance function as presented in Appendix 2. The dispersion measure is now

$$v_{\Delta g}^2 = C_o - \tilde{M}^T H^{-1} \tilde{M} \ ,$$

which corresponds to a diagonal element of $M\{\tilde{\epsilon}\tilde{\epsilon}^T\}$; $C_o \equiv C(0)$ in this expression is obtained from the covariance function for gravity anomalies.

6.3 Collocation Algorithm

The formulas for the L.S. collocation with noise can be developed in a close analogy to the best linear prediction method of Appendix 2. The basic difference between the two approaches resides in the statistical nature attributed to the observations. In particular, in the present approach the observations are no longer considered as errorless quantities. Thus, in addition to the symbol M (averaging operator over the unit sphere) introduced in the beginning paragraph of Appendix 2, also the symbol E (mathematical expectation operator) would have to be considered in the derivations. In adapting the development of Appendix 2 to the present context, one can imagine the operator M replaced by the operator $\overline{M}$. The latter represents both of the operators E and M taken together in either order (due to their independence), symbolized by

$$\overline{M} \equiv EM \equiv ME .$$

With the above stipulation the formulas of Appendix 2 can be easily modified. In particular, the errorless vector F in (A2.7-9) is replaced by F^b, where

$$F^b = F + e ,$$

and where e is the vector of observational noise whose variance-covariance matrix is

$$E\{ee^T\} \equiv \Sigma .$$

From the nature of the operators E and M, described in [Moritz, 1980], it follows that

$$E\{P\} = P \ , \qquad E\{F\} = F \ , \qquad E\{e\} = 0 \ ,$$

$$M\{P\} = 0 \ , \qquad M\{F\} = 0 \ , \qquad M\{e\} = e \ .$$

As further consequences, we have

$$\overline{M}\{PP^T\} = M\{PP^T\} \ ,$$

$$\overline{M}\{F^b P^T\} = \overline{M}\{FP^T\} + \overline{M}\{eP^T\}$$

$$\equiv M\{FP^T\} + E\{e\}M\{P^T\} \equiv M\{FP^T\} \ ,$$

$$\overline{M}\{F^b F^{bT}\} = \overline{M}\{FF^T\} + \overline{M}\{Fe^T\} + \overline{M}\{eF^T\} + \overline{M}\{ee^T\}$$

$$\equiv \overline{M}\{FF^T\} + \overline{M}\{ee^T\} \equiv M\{FF^T\} + E\{ee^T\} \ . \tag{6.8}$$

With the above changes, (A2.9) in the present context would read as it stands except that M on the left-hand side would be replaced by $\overline{M}$, and $M\{FF^T\}$ on the right-hand side would have $E\{ee^T\}$ added to it. This last change would take place also in (A2.10-12); in addition, the vector F in (A2.11) would be replaced by F^b and the operator M on the left-hand side of (A2.12) would be replaced by $\overline{M}$. Upon denoting the "error measure" as described through $\overline{M}$ just mentioned by the symbol C, the final results corresponding to (A2.11'), (A2.12') and the remainder of that paragraph in Appendix 2 would now read

$$\hat{P} = M^T(H + \Sigma)^{-1} F^b \equiv M^T W \ , \tag{6.9}$$

$$C_{\hat{P}} = H_p - M^T(H + \Sigma)^{-1} M \ , \tag{6.10}$$

where

$$W \equiv (H+\Sigma)^{-1}F^b \; ;$$

$$H \equiv M\{FF^T\} \; , \qquad \Sigma \equiv E\{ee^T\} \; ;$$

$$M^T \equiv M\{PF^T\} \; , \qquad H_P \equiv M\{PP^T\} \; .$$

Equations (6.9) and (6.10) are essentially the formulas (14-27) and (14-42) in [Moritz, 1980], characterizing the L.S. collocation with noise.

With regard to the predictions $\tilde{P}$ symbolizing functions of different kind from F, the results corresponding to (A2.11″) and (A2.12″) in Appendix 2 would similarly become

$$\hat{\tilde{P}} = \tilde{M}^T(H + \Sigma)^{-1}F^b \equiv \tilde{M}^T W \; , \tag{6.11}$$

$$C_{\hat{\tilde{P}}} = H_{\tilde{P}} - \tilde{M}^T(H+\Sigma)^{-1}\tilde{M} \; , \tag{6.12}$$

with the additional notations

$$\tilde{M}^T \equiv M\{\tilde{P}F^T\} \; , \qquad H_{\tilde{P}} \equiv M\{\tilde{P}\tilde{P}^T\} \; .$$

The discussion in the paragraphs following (A2.15) in Appendix 2 would now be somewhat changed. If all the prediction points coincided with the (n) observation points, it would similarly hold true that

$$M^T = H \; , \qquad H_P = H \; ;$$

but from (6.9) and (6.10), upon changing "$\hat{P}$" to "$\hat{F}$", it would now follow:

$$\hat{F} = H(H + \Sigma)^{-1}F^b , \qquad (6.13)$$

$$C_{\hat{F}} = H - H(H + \Sigma)^{-1}H . \qquad (6.14)$$

These equations no longer yield F^b and 0, respectively, as in Appendix 2, but the results will approach such values as Σ approaches 0.

In the case where one prediction point (J) coincides with the one and only observation point (when n=1), equations (6.13) and (6.14) become

$$\hat{F}_J = [D_o/(D_o + \sigma^2)]F_J^b ,$$

$$\sigma_{\hat{F}_J}^2 = D_o - D_o^2/(D_o + \sigma^2) ,$$

where the variance-covariance matrix Σ reduces to the variance σ^2. If $\sigma^2 << D_o$, the above relations reveal that

$$\hat{F}_J \simeq (1 - \sigma^2/D_o)F_J^b ,$$

$$\sigma_{\hat{F}_J}^2 \simeq \sigma^2 .$$

Thus F_J^b is not reproduced exactly, but is reduced by the (small) factor σ^2/D_o. Here again, as σ^2 goes to zero the previous results are recovered.

Instead of being based on the S.H. potential coefficients, the formulas for c_n , d_n and h_n in Appendix 2 can be developed with the aid of the closed-form expressions from [Tscherning and Rapp, 1974], adapted on pages 76 and 77 of [Blaha, 1982]. For the k-th degree variances we then have

$$c_k = s^{k+2}A(k-1)/[(k-2)(k+B)] ,$$

$$d_k = c_k R^2/[G^2(k-1)^2] ,$$

$$h_k = c_k R/[G(k-1)] = d_k G(k-1)/R ,$$

with

$$s = 0.999617 \ ,$$

$$A = 425.28 \text{ mgal}^2 \ ,$$

$$B = 24 \ ,$$

and with $R = 6.371 \times 10^6$ m representing the earth's mean radius and $G = 979.8$ gal representing the average value of gravity on the earth's surface.

In the final formulas below the degree n represents the smallest features of the earth's gravity field taken into account by the known S.H. expansion and C, D, H represent the (cross-) covariance functions due to the neglected degrees:

$$c_k = 0.999617^{k+2} \times (k-1) \times 425.28 \text{ mgal}^2 / [(k-2)(k+24)] \ , \tag{6.15}$$

$$d_k = 0.999617^{k+2} \times 17,981 \text{ m}^2 / [(k-1)(k-2)(k+24)] \ , \tag{6.16}$$

$$h_k = 0.999617^{k+2} \times 2,765.3 \text{ mgal} \times \text{m} / [(k-2)(k+24)] \ ; \tag{6.17}$$

$$C(\psi) = \sum_{k=n+1}^{\infty} c_k P_k(\cos\psi) \ , \qquad C(0) = \sum_{k=n+1}^{\infty} c_k \ , \tag{6.18}$$

$$D(\psi) = \sum_{k=n+1}^{\infty} d_k P_k(\cos\psi) \ , \qquad D(0) = \sum_{k=n+1}^{\infty} d_k \ , \tag{6.19}$$

$$H(\psi) = \sum_{k=n+1}^{\infty} h_k P_k(\cos\psi) \ , \qquad H(0) = \sum_{k=n+1}^{\infty} h_k \ . \tag{6.20}$$

We note that (6.18-20) could be computed using, for example, the closed forms appearing on pages 44, 45 of [Tscherning and Rapp, 1974]. But if the practical computation proceeds as indicated in (6.18-20), the symbol "∞" can be

replaced by a sufficiently large number such as 500 or 1,000, etc. With the above values of the functions C,D and H, the matrices H, M^T and H_p needed in (6.9) and (6.10), as well as the matrices $\tilde{M}^T$ and $H_{\tilde{p}}$ needed in (6.11) and (6.12), can be formed as in Appendix 2, equations (A2.13-15) including the remainder of that paragraph.

The theory just described is first considered in view of the predictions of geoid undulations, where the observed quantities, F^b, are the geoid undulations referring to the S.H. model truncated at (n,n) degree and order. These observations are typically the (minus) geoidal residuals from a S.H. adjustment of satellite altimetry. The formulas (6.9) and (6.10) are now rewritten as

$$\hat{P} = M^T \tilde{H}^{-1} F^b \,, \tag{6.21}$$

$$C_{\hat{P}} = H_P - M^T \tilde{H}^{-1} M \,, \tag{6.22}$$

where

$$F^b = F + e \,, \tag{6.23}$$

$$\tilde{H} = H + \Sigma \,. \tag{6.24}$$

Here F is the vector of "true" values of geoid undulations referring to the (n,n) field, i.e., of values owing their existence to the truncated degrees from n+1 to infinity, while e is the observational noise (independent of F). The matrix H corresponds to the vector F, in the sense that "n" in the covariance function $D(\psi)$ used in forming H according to the locations of the observation points is the same as the "n" of the (n,n) field associated with the values in F. In the same vein the matrix M^T corresponds to F as well, while the matrix

-64-

Σ corresponds to the vector e. The matrix H_p corresponds to $\hat{P}$ and thus to the locations of the prediction points, but $D(\psi)$ and "n" used in its construction are the same as above.

Next consider a practical case in which the predictions are required to describe a smooth geoid. Such a geoid can be represented by a S.H. expansion (n',n'), as opposed to the theoretical expansion (∞,∞). For example, a 1^0-geoid would correspond roughly to a (180,180) S.H. expansion. In this task, the "true" geoid is assumed to be described perfectly by a (n',n') S.H. expansion, all the other S.H. potential coefficients being considered as zeros. With regard to such a geoid, the above formulas would be unchanged except that the symbol ∞ in the expression for $D(\psi)$ would be replaced by n'. However, an inconsistency would manifest itself in a real-world situation where F refers to the actual (unsmooth) geoid as sensed through the observations F^b. Therefore, the adaptation of $D(\psi)$ to the "true" geoid under consideration is equivalent to modeling only the corresponding F'-part of F as errorless values and pushing the remaining part, F'', into the realm of "errors", namely

$$F = F' + F'' . \qquad (6.25)$$

The observational vector is thus split as follows:

$$F^b = F' + (F'' + e) , \qquad (6.26)$$

or

$$F^b = F' + e' , \qquad (6.27)$$

$$e' = F'' + e . \qquad (6.28)$$

The problem of the L.S. collocation with noise is now reformulated in a slightly modified fashion. One is to find the best linear estimate $\hat{P}'$,

$$\hat{P}' = A'^T F^b , \tag{6.29}$$

where the matrix A' is unknown. The primes indicate that the "true" geoid corresponds to the highest degree n' and not to ∞ which would characterize the unprimed quantities. In analogy to Appendix 2, the problem of finding A'^T is addressed through the operator $\overline{M}$. With $\varepsilon'=P'-\hat{P}'$, one forms the "dispersion matrix",

$$\varepsilon'\varepsilon'^T = P'P'^T - P'F^{bT}A' - A'^T F^b P'^T + A'^T F^b F^{bT} A' ,$$

and its "average" as

$$\overline{M}\{\varepsilon'\varepsilon'^T\} = \overline{M}\{P'P'^T\} - \overline{M}\{P'F^{bT}\}A' - A'^T\overline{M}\{F^b P'^T\} + A'^T\overline{M}\{F^b F^{bT}\}A' . \tag{6.30}$$

Upon considering the nature of the operators M and E as in [Moritz, 1980], it follows for the first term on the right-hand side of (6.30):

$$\overline{M}\{P'P'^T\} = M\{P'P'^T\} . \tag{6.31}$$

The second term (and thus also the third term) is first developed according to (6.27) as

$$\overline{M}\{P'F^{bT}\} = \overline{M}\{P'F'^T\} + \overline{M}\{P'e'^T\} . \tag{6.32}$$

Similar to (6.31), we have

$$\overline{M}\{P'F'^T\} = M\{P'F'^T\} . \tag{6.33a}$$

On the other hand, in considering (6.28) it follows that

$$\overline{M}\{P'e'^T\} = \overline{M}\{P'F''^T\} + \overline{M}\{P'e^T\} = M\{P'F''^T\} + M\{P'\}E\{e^T\} \equiv M\{P'F''^T\} \ .$$

But this last matrix is zero as is immediately apparent from page 256 of [Heiskanen and Moritz, 1967]. In particular, the elements of P' can be expressed via a S.H. expansion in degrees n+1 through n' , and the elements of F" can similarly be expressed in degrees n'+1 through ∞. Thus any element of $P'F''^T$ contains a sum of products in which only different degrees are present. Due to the average product (under the operator M) of two Laplace harmonics of different degrees being zero, it follows that

$$M\{P'F''^T\} = 0 \ , \tag{6.33b}$$

and, similarly,

$$M\{F'F''^T\} = 0 \ . \tag{6.33c}$$

With (6.33a,b) equation (6.32) becomes

$$\overline{M}\{P'F^{bT}\} = M\{P'F'^T\} \ . \tag{6.34}$$

In considering (6.27) and (6.28), we develop

$$\overline{M}\{F^bF^{bT}\} = \overline{M}\{F'F'^T\} + \overline{M}\{F'e'^T\} + \overline{M}\{e'F'^T\} + \overline{M}\{e'e'^T\} \ , \tag{6.35}$$

where, similar to (6.31) and (6.33a),

$$\overline{M}\{F'F'^T\} = M\{F'F'^T\} \ .$$

Furthermore,

$$\overline{M}\{F'e'^T\} = \overline{M}\{F'F''^T\} + \overline{M}\{F'e^T\} \equiv M\{F'F''^T\} + M\{F'\}E\{e^T\} = 0 \ ,$$

-67-

where use was made of (6.33c). Finally, we have

$$\overline{M}\{e'e'^T\} = \overline{M}\{F''F''^T\} + \overline{M}\{F''e^T\} + \overline{M}\{eF''^T\} + \overline{M}\{ee^T\} \equiv M\{F''F''^T\} + E\{ee^T\} .$$

Upon collecting the last three results, (6.35) yields

$$\overline{M}\{F^bF^{bT}\} = M\{F'F'^T\} + M\{F''F''^T\} + E\{ee^T\} . \qquad (6.36a)$$

This can also be written as

$$\overline{M}\{F^bF^{bT}\} = M\{FF^T\} + E\{ee^T\} , \qquad (6.36b)$$

due to the fact that

$$M\{FF^T\} = M\{F'F'^T\} + M\{F'F''^T\} + M\{F''F'^T\} + M\{F''F''^T\} \equiv M\{F'F'^T\} + M\{F''F''^T\} ,$$

where (6.33c) has been utilized. It is thus confirmed that the matrix in (6.36a) is the same as that expressed by (6.8).

In applying (6.31), (6.34) and (6.36b) to (6.30), we have

$$\overline{M}\{\epsilon'\epsilon'^T\} = M\{P'P'^T\} - M\{P'F'^T\}A' - A'^TM\{F'P'^T\} + A'^T(M\{FF^T\} + E\{ee^T\})A' .$$

This is written as

$$\overline{M}\{\epsilon'\epsilon'^T\} = H_{p'} - M'^TA' - A'^TM' + A'^T(H + \Sigma)A' , \qquad (6.37)$$

where the new notations are

$$M'^T \equiv M\{P'F'^T\} , \qquad H_{p'} \equiv M\{P'P'^T\} .$$

Again in analogy to Appendix 2, the matrix in (6.37) should have a minimum trace. In particular, if one applies the operator "Tr" and differentiates with respect to A'^T, the result has to be a zero matrix:

$$\partial Tr[H_{p'}]/\partial A'^T - 2\partial Tr[A'^T M']/\partial A'^T + \partial Tr[A'^T(H + \Sigma)A']/\partial A'^T = 0.$$

The rules for differentiation of traces yield

$$0 - 2M'^T + 2A'^T(H + \Sigma) = 0 ,$$

and thus

$$A'^T = M'^T(H + \Sigma)^{-1} .$$

It now follows from (6.29) and (6.37) that

$$\hat{p}' = M'^T \tilde{H}^{-1} F^b ,\tag{6.38}$$

$$C_{\hat{p}'} = H_{p'} - M'^T \tilde{H}^{-1} M' ,\tag{6.39}$$

where $\tilde{H}$ has the same meaning as in (6.24). We may add that with the self-evident changes in notations, (6.36a) allows $\tilde{H}$ to be also expressed as

$$\tilde{H} = H' + (H'' + \Sigma) ,$$

which corresponds to the splitting in (6.26), in analogy to the correspondence between (6.23) and (6.24). In comparing (6.21) and (6.22) with (6.38) and (6.39), we see that the only difference between the formulas pertaining to the actual geoid and the smoothed geoid resides in replacing M^T and H_p in the former by M'^T and H'_p ; this is accomplished simply by replacing "∞" (in practice 1,000, etc.) by n' in conjunction with $D(\psi)$. As has been already indicated, the matrix $\tilde{H}$ given in (6.24) is unchanged, i.e., the computation proceeds with "∞".

Besides the computational shortcut, the above procedure is compatible with expressing the geoid through the S.H. expansion to the degree and order (n',n').

-69-

In particular, one can utilize the predicted values $\hat{P}'$ distributed in an appropriate (equilateral) grid and compute the S.H. potential coefficients via integral formulas. If "unsmoothed" values $\hat{P}$ were utilized instead, the smoothing would occur at the level of these coefficients. As a final remark, we observe that the above derivation is general, in the sense that the "unsmoothed" formulas (6.21) and (6.22) follow from (6.38) and (6.39) simply by replacing n' by ∞ as a special case.

One of the final products we wish to form, using the geoidal predictions obtained via the modified L.S. collocation with noise as has just been described, is represented by contour maps of (smoothed) geoid undulations and gravity anomalies over the oceanic regions covered by satellite altimetry. The resolution implied by such maps corresponds to the density of the prediction points and to the smoothness of the predictions implied by the degree n'. Clearly, these two characteristics should be consistent with each other. Thus, if n' corresponds to a 2^0 geoidal resolution, the prediction points should form a $2^0 \times 2^0$ equilateral grid, not a coarser grid. A finer grid would not detract from the resolution displayed by a contour map but would be uneconomical, depending on its interval and other characteristics (e.g., a $1^0 \times 1^0$ geographical grid would be wasteful compared to a $1^0 \times 1^0$ equilateral grid which, in turn, would be wasteful compared to a $2^0 \times 2^0$ equilateral grid). The appropriate size of the grid can also serve as a guidance when determining a useful size of the neighborhood (around a given prediction point) supplying the data values F^b in (6.38); for example, observation points removed several grid intervals from this prediction point would have little effect on the predicted value and could be left out of the computation.

-70-

We now focus our attention on developing the procedure for drawing geoidal and gravity anomaly maps consistent with the resolution implied by n', such as a 2^0 resolution. Given a $2^0 \times 2^0$ equilateral grid of predicted geoid undulations referring to the (n,n) field, various interpolation techniques could be used to fill in the undulations at intermediate points as needed by a particular contour routine. For example, a polynomial interpolation could be used for this purpose (some contour routines themselves use this type of interpolation). The intermediate, or densifying, points could be chosen to form a $1^0 \times 1^0$ geographical grid from which a geoidal map could be drawn in the Mercator projection, etc. It is understood that all the predicted geoid undulations should be added algebraically to the undulations computed through the (n,n) S.H. expansion in order to arrive at the final geoid undulations corresponding to the (n',n') field.

A suitable interpolation technique yielding the desired densifying grid is the best linear prediction method, or errorless collocation, described in Appendix 2. Indeed, all we wish to accomplish at this point is to densify the original (equilateral) grid of predicted values considered as perfect in view of contour lines. Quite naturally, the smoothness in the filled-in values should correspond to the smoothness in the original predictions. This requirement is satisfied if the n' adopted for $D(\psi)$ in the errorless collocation is the same as the n' used previously in the modified L.S. collocation with noise when formulating the matrices M'^T and $H_{p'}$. Such a simple relationship between the densifying method and the original prediction method -- fulfilling the need for uniform resolution characteristics -- demonstrates the suitability of the errorless collocation for the task at hand.

-71-

In accordance with the above discussion, the following prediction algorithm can be used for grid densifications:

$$\hat{\tilde{P}}' = \tilde{M}'^T H_{P'}^{-1} \hat{P}' \quad , \qquad (6.40)$$

$$C_{\hat{\tilde{P}}'} = H_{\tilde{P}'} - \tilde{M}'^T H_{P'}^{-1} \tilde{M}' \quad , \qquad (6.41)$$

where the symbol "~" indicates the densified geoid undulations. In this case $\hat{P}'$ in (6.40) designates the vector of predicted values obtained in (6.38) and $H_{P'}$ in (6.40) and (6.41) designates the matrix which appeared in the same notation on the right-hand side of (6.39). The matrices $\tilde{M}'^T$ and $H_{\tilde{P}'}$ are formed according to the locations of the densifying points via the covariance function $D(\psi)$. If a densifying point coincides with an original prediction point, the original predicted quantity is exactly reproduced by this method (see Appendix 2), which is a desired interpolation characteristic from the standpoint of contour lines.

But the equations of the type (6.40) and (6.41) can be used for grid densifications in terms of other geophysical quantities as well. Assume first that (6.38) and (6.39) have been used for smoothed out predictions of gravity anomalies, in which case the covariance function $D(\psi)$ serving in the formation of M'^T and $H_{P'}$ has been replaced by the cross-covariance function $H(\psi)$ and the covariance function $C(\psi)$, respectively. Next assume, for a moment, that the notations in (6.38) and (6.39) are retained also in this new situation. It then follows that the last three sentences of the preceding paragraph can be repeated as they stand also with regard to the densifications of gravity anomalies, except that $C(\psi)$ replaces $D(\psi)$.

The values which could serve in evaluating the effectiveness and the resolution power of the final product are the residuals computed with respect to the geoidal contour map. One could locate a specific observation point on

the map, estimate its geoid undulation referring to the (n,n) field, and compute the difference between this value and its counterpart in F^b. However, such an estimated undulation can be found much more easily upon using the same procedure that has led to the construction of the geoidal contour lines themselves. In particular, the formula (6.40) can be used in this task, where the observation points are treated exactly in the same fashion as the densifying points. In practice, only a limited area associated with the values $\hat{P}'$ is considered around the observation point, similar to the procedure mentioned earlier with regard to the neighborhood containing the observations F^b. Quite logically, the size of the area used in the residual computation should be compatible with its counterpart in the densification (6.40); the approximations committed in computing the residuals will thus be compatible with the approximations embodied in the construction of the contour lines.

6.4 Practical Considerations

At the outset we recall two phases of the L.S. adjustment used at AFGL in satellite altimetry reductions: the first, spherical-harmonic adjustment yields a smoothed out global geoid, and the second, point-mass adjustment results in a more detailed geoid on a local or a large-scale basis. The residuals computed after both adjustment phases contain, in addition to a random component (due to observational noise and unmodeled tidal and other effects), also unaccounted for short-wavelength geoidal information.

These residuals can be exploited in their own right. For example, upon using some approximate procedure they could be translocated to form a postulated grid and then treated by various computationally efficient techniques to yield a "third-phase" (detailed) resolution. However, the collocation approach presented in Section 6.3 can also lead to such a third-phase resolution, and can be used on a local, regional, or global basis. Furthermore, it yields error estimates associated with the predicted quantities. Clearly, this technique can be based directly on the residuals from the global adjustment as in the second-phase resolution which, so far, has been accomplished through the point-mass adjustment. The principle of the collocation application remains the same for either choice, i.e., for the second-phase or the third-phase resolution.

From the conceptual point of view, the second- or third-phase collocation process could be called an "observation domain" solution since the output quantities are of the same kind as the input quantities, namely the geoid undulations. With the aid of the appropriate cross-covariance function, the geoid

undulations can be subsequently transformed into gravity anomalies, etc. We recall that this approach does not use intermediate parameters such as the point-mass magnitudes computed as a part of the previous second-phase L.S. adjustment process.

Using the altimeter data entails some practical difficulties which could hinder the efficiency of the collocation technique from the standpoint of both the computer storage and run-time requirements. Most notable in this respect is the presence of a great many observation points within small oceanic areas. In addition to the computer burden, this phenomenon could also cause numerical problems during the inversion of the matrix designed as $\tilde{H}$ in Section 6.3. In particular, if any two observation points were located in close proximity to each other, $\tilde{H}$ could become ill-conditioned, especially if the noise level represented by the matrix Σ is low.

The above difficulties can be circumvented by using the algorithm developed in Appendix 3, which could be viewed as a specific kind of translocation. It performs a weighted averaging of the location of two observation points situated closer together than a pre-determined limit, as well as the same weighted averaging of the corresponding geoidal residuals (the latter form F^b of Section 6.3, i.e., the input for the collocation predictions). If the resulting observation point is too close to some other, a similar process again takes place. However, instead of averaging the geographic coordinates ϕ and λ, the algorithm gives directly the desired trigonometric functions. Thus, instead of nine columns per observation point only seven columns are needed in a "storage" matrix whose rows correspond to the number of the prediction points. The locations of the prediction points are usually stipulated beforehand; as we have seen earlier, it is advisable that they form an equilateral grid.

The elimination of the above two columns -- which are not needed in the actual prediction process -- allows for the inclusion of more prediction points and/or more observation points per prediction point than would otherwise be possible in a computer run. The savings amount to about 29% of the above "storage" matrix which has by far the greatest storage requirements of the entire collocation application. The basic seven columns mentioned in the last paragraph represent the following information: $\cos\phi_i$, $\sin\phi_i$, $\cos\lambda_i$, $\sin\lambda_i$, $\cos\psi_{Ji}$, $\sin\psi_{Ji}$ and N_i, where the index J pertains to a specific prediction point and the index i pertains to the observation point whose input geoid undulation (more precisely, the part unmodeled by the previous adjustment plus the observational noise) is N_i.

The observation points i are arranged according to their angular distance (ψ) from the prediction point J, so that the point No. 1 is closer to J than is the point No. 2, etc. If neither of the considered points has been averaged before, the respective weight factors are taken as unity. If a point has been averaged once before and if another averaging is to take place, its weight factor is 2. Except for the weight factor, the weight is in reverse proportion to the (angular) distance between the observation point and its prediction point. This importance given to the distance is rooted in the consideration of the prediction formula where the contribution of individual observation points diminishes quite rapidly with distance from the prediction point, reflecting the behavior of the covariance function.

As has been already pointed out in Section 6.3 the basic, or original, predictions are considered to form an equilateral grid. Such a distribution gives rise to a uniform resolution depending on the grid interval (the degree n' defined in the same section is assumed to be compatible with this interval).

Accordingly, a unit sphere representing the globe is thought of as subdivided into compartments, each characterized by the appropriate angular intervals $\Delta\phi$ and $\Delta\lambda$, and each associated with one centrally located prediction point. The value of $\Delta\phi$ is independent of position, but the value of $\Delta\lambda$ varies as $\Delta\phi/\cos\phi$, where ϕ is the geocentric latitude. The poles would be an exception to this rule (the compartments would become spherical caps), but they are omitted from this development. In the case of SEASAT, for example, the ground tracks reach only the latitudes $\pm72°$ beyond which no predictions are made. The continental areas with no altimeter measurements are likewise ignored in the current application.

Although in theory all the observation points should be involved in any prediction, in practice such a procedure would be extremely wasteful. Due to the nature of the geoidal covariance function, the observation points represented by the vector F^b can be restricted to a relatively small neighborhood of the pertinent prediction point (called J). Clearly, all the observation points from the compartment represented by J should be involved. However, the question of how far beyond this compartment the search for observation points should be extended is a matter of judgment and experience, depending to a large extent on the cmputer characteristics and limitations.

Practical considerations coupled with numerical evaluations have indicated that the inclusion of observation points located within the spherical cap that just covers the corners of the compartment J is reasonable. This provides for a modest measure of continuity between neighboring predictions because of the overlap in peripheral observations. The radius of such a cap, centered at J, is approximately $0.75\Delta\phi$. Even so, the number of observation points involved in one prediction may sometimes be prohibitive. This occurs in spite of the

-77-

input data being limited to 0.5°-intervals along satellite arcs, and is due to a substantial increase in the number of observations brought about by the presence of repeating tracks. It then becomes necessary to stipulate a maximum allowable number of observation points and discard the points farthest away from J until this limit is satisfied. For this reason it is useful to have the observation points ordered according to their angular distances (ψ) from J.

The number of observation points within the spherical cap introduced above depends, of course, on the desired resolution. In a 2° resolution (the grid size corresponds to $\Delta\phi=2°$) the number of observations often reaches beyond 50. In a 1° resolution this number is likely to decrease four-fold. If the limit in the former case is set to 50-60, most of the observations within the pertinent cap will be accepted. On the other hand, the limit of 20-30 in the latter case will often result in all of the observations being accepted. These limits serve merely as practical guidelines. Clearly, the final number of observation points is also reduced by the special translocation (averaging) technique described in the first part of this section. In this respect, the minimum separation limit of $0.2\Delta\phi$ has proven useful.

With regard to the densifying points, it is suggested that the spherical cap centered at any such point be enlarged to over $1\Delta\phi$ (e.g., $1.125\Delta\phi$ has been used satisfactorily). This suggestion stems from the fact that only relatively few prediction points, represented by the vector $\hat{P}'$ in (6.40), are located around any densifying point. Similar to an earlier statement, the points where the "residuals" are sought should again be treated in the manner of densifying points.

Orbital considerations dictate that the finest grid of prediction points to be used in conjunction with SEASAT observations is a $1^0 \times 1^0$ equilateral grid. This limitation is imputable to the ground tracks intersecting in a very approximate equilateral grid with about 1^0 on the side over much of the oceanic surface. The contour maps could thus represent a 1^0 resolution at best, which is understood as expressing the features down to and including those whose shortest half-wavelength is 1^0. Since such a resolution corresponds approximately to a (180,180) set of S.H. potential coefficients, the truncation n' used in Section 6.3 in conjunction with the covariance and cross-covariance functions is approximately n'=180.

Finally, we note that the predictions described herein can be considered as "best", but only when viewed as a whole, i.e., on the global scale. This stems from the global character of the covariance and cross-covariance functions characteristic of the M-averaging as presented in Appendix 2 and as used in Section 6.3. If a similar procedure should be applied on a regional basis, regional covariance and cross-covariance functions as well as regional averaging would have to be employed in order to yield some "best" predictions on a smaller scale. If such regional functions -- or any other functions different from those in Appendix 2 -- were used for predictions covering the entire globe, the quality of these predictions as a whole would necessarily be worse than the quality of the predictions dealt with herein.

7. CONCLUSIONS

The topics addressed in this report have separate characteristics. They are treated in Chapters 2-6 which are essentially self-contained. Accordingly, only a brief summary of most topics is presented below.

In Chapter 2, a classical oceanographic procedure is justified by showing that except for a factor, the pressure gradient along equipotential surfaces is interchangeable in practice with the geopotential gradient along isobaric surfaces. The use of the normal coordinate system allows the assessment of the approximations involved in such a practical formulation, as well as the development of the rigorous formulation with an additional factor containing dW/g, where W is the geopotential and g is the gravity. Except for the geopotential considered as increasing downward according to the geodetic convention, the tensor notations and concepts of [Hotine, 1969] are adhered to.

Chapter 3 takes advantage of the formula for the bottom tide as developed in [Schwiderski, 1980] and in other reports by the same author. Although these reports do not deal with altimeter adjustment per se, an improvement of the altimeter model with tidal effects is achieved through the replacement of the approximate value of the ocean bottom deformation due to ocean tidal loading by a more rigorous formulation. As an additional advantage, this formulation can be used in conjunction with all of the tidal constituents.

In Chapter 4, an economical yet quite rigorous weighting scheme is developed for altimeter observations in the first-phase adjustment. It is based on the first-order autoregressive process of [Brown and Trotter, 1969] applied to the values obtained with the geoidal covariance function. Its

main outcome is represented by a tri-diagonal weight matrix which, when compared to the rigorous case of a fully populated weight matrix, offers almost the same level of computer economies as a diagonal weight matrix. However, the errors associated with a diagonal matrix are greatly reduced in this approach, perhaps by 60%.

Chapter 5 extends the concept of second-phase adjustment of satellite altimetry by incorporating chosen tidal parameters in the point-mass model. Although the point masses in a given ocean basin receive in general different adjustment corrections, it is not so for the tidal parameters considered common to the whole area. These parameters are now associated with the border of the matrix of normal equations. Accordingly, whereas the "modified Choleski algorithm" of [Blaha, 1983] containing the point-mass parameters alone corresponds to a banded *system of normal* equations, the new "extended modified Choleski algorithm" results in a banded-bordered system of normal equations. In the closing part of Chapter 5 it is confirmed that the former is a special case of the latter. In either case, the presented algorithm is computationally efficient.

Finally, Chapter 6 offers an alternative to a second- or third-phase simultaneous least-squares adjustment process. In particular, Section 6.3 contains an approach based on the development of the collocation theory as presented in [Heiskanen and Moritz, 1967] and [Moritz, 1980]. Both the signal and the noise are considered to be present at any observation point, and are associated with the averaging operators M and E, respectively. The derivations proceed strictly in matrix notations. It is shown that if the predicted values of geophysical quantities should be desired in a smoothed

out version, the standard collocation approach is unchanged except that during the formation of the first matrix in the prediction formula, the covariance (or cross-covariance) function is no longer utilized in conjunction with the expansion degree "∞", but only in conjunction with the degree n' corresponding to the required smoothness. As n' increases, the standard "unsmoothed" collocation version is seen to follow from its smoothed out counterpart as a special case.

A somewhat more detailed summary of the most important outcome of Section 6.3 is deemed useful (without the re-introduction of the notations utilized therein). With

$$\tilde{H} = H + \Sigma ,$$

equations (6.21) and (6.22) are recapitulated as

$$\hat{P} = M^T \tilde{H}^{-1} F^b ,$$

$$C_{\hat{P}} = H_P - M^T \tilde{H}^{-1} M .$$

The matrices M^T, H and H_P are formed using the covariance function $D(\psi)$ corresponding to (the signal part of) F^b. The latter consists here of geoid undulations, but this case can be generalized with minimal and self-evident changes.

With regard to geophysical quantities other than those represented by F^b, one can go over the derivations leading to the above formulas and add the symbol "~" to all the vectors and matrices except F^b, H, Σ (and W if it should be used). The result is

$$\hat{\tilde{P}} = \tilde{M}^T \tilde{H}^{-1} F^b ,$$

$$C_{\hat{\tilde{P}}} = H_{\tilde{P}} - \tilde{M}^T \tilde{H}^{-1} \tilde{M} .$$

In the current application the desired quantities are gravity anomalies; the matrix $\tilde{M}^T$ is thus formed using the cross-covariance function $H(\psi)$ and $H_{\tilde{P}}$ is formed using the covariance function $C(\psi)$.

Equations (6.38) and (6.39) pertaining to the smoothed out predictions are recapitulated as

$$\hat{P}' = M'^T \tilde{H}^{-1} F^b ,$$

$$C_{\hat{P}'} = H_{P'} - M'^T \tilde{H}^{-1} M' .$$

The matrices M'^T and $H_{P'}$ are computed as their unprimed counterparts except that the degree "∞" in the formation of $D(\psi)$ is replaced by n'. As n' increases to infinity, these formulas become their unprimed counterparts.

If one seeks the smoothed out predictions of geophysical quantities other than those represented by F^b, in analogy to the case already treated one can go over the derivations and add the symbol "~" to all the vectors and matrices except F^b, H, Σ (and W if it should be used). The result is

$$\hat{\tilde{P}}' = \tilde{M}'^T \tilde{H}^{-1} F^b ,$$

$$C_{\hat{\tilde{P}}'} = H_{\tilde{P}'} - \tilde{M}'^T \tilde{H}^{-1} \tilde{M}' .$$

The matrices $\tilde{M}'^T$ and $H_{\tilde{P}}$ are computed as their unprimed counterparts except that the degree "∞" is again replaced by n'. As n' increases to infinity,

these formulas become their unprimed counterparts. One notices that the vector $\tilde{H}^{-1}F^b \equiv W$ is unchanged in all four prediction formulas above.

Section 6.3 also demonstrates that the densifications of the predicted geophysical quantities, needed especially in view of contour maps, can proceed with advantage upon using the errorless collocation. The effectiveness of the presented approach in its entirety can be evaluated with the aid of the residuals (at observation points) computed with respect to the geoidal contour map. Here the errorless collocation represents not only a useful but also a consistent tool, due to the fact that it has lead to the construction of the geoidal contour map itself.

APPENDIX 1

COMPUTER PROGRAM FOR GEOIDAL VARIANCE-COVARIANCES
DUE TO TRUNCATIONS
IN THE UNDERLYING SPHERICAL-HARMONIC MODEL

```
C
      PROGRAM CNTRL (INPUT, OUTPUT, TAPE5=INPUT, TAPE6=OUTPUT)
C     COMPUTE VARIANCE-COVARIANCES (IN METERS SQUARE) DUE TO TRUNCATIONS
C     OF THE SPHERICAL-HARMONIC MODEL FOR GEOID UNDULATIONS
C
      COMMON/ORDER/IORDER
      COMMON/COSPSI/ZED
      COMMON/PLEG/PZ(1000)
      DIMENSION DEGVAR(1000)
      DIMENSION PSI(30)
      DIMENSION N(20)
      DIMENSION SM(20,30)
      DATA ZER, RAD/0.,0.01745329252/
      LOGIN = 5
      LGOUT = 6
C
      WRITE(LGOUT,5)
      IZ = 0
      READ(LOGIN,15) NPROB
    1 IZ = IZ + 1
      WRITE(LGOUT,25) IZ
      READ(LOGIN,15) IORDER
      IF(IORDER.GT.1000) IORDER = 1000
      ..RITE(LGOUT,35) IORDER
      READ(LOGIN,15) NPSI
      WRITE(LGOUT,45) NPSI
      READ(LOGIN,55)(PSI(I),I = 1,NPSI)
      WRITE(LGOUT,55)(PSI(I),I = 1,NPSI)
      DO 2 I = 1,NPSI
    2 PSI(I) = RAD*PSI(I)
      READ(LOGIN,15) NN
      WRITE(LGOUT,65) NN
      READ(LOGIN,15)(N(J),J = 1,NN)
      WRITE(LGOUT,15)(N(J),J = 1,NN)
C
      DEGVAR(1) = ZER
      DEGVAR(2) = ZER
      DO 3 K=3,IORDER
      XKM1 = K - 1
      XKM2 = K - 2
      XKP24 = K + 24
      KP2 = K + 2
      DEGVAR(K) = (0.999617**KP2)*17981./(XKM1*XKM2*XKP24)
    3 CONTINUE
```

```
C
      DO 4 I = 1,NPSI
      ZED = COS(PSI(I))
      CALL LEGEN
      K = IORDER + 1
      SUM = ZER
      IPART = NN + 1
    6 CONTINUE
      IPART = IPART - 1
      NPART = N(IPART)
    7 CONTINUE
      K = K - 1
      IF(K.EQ.NPART) GO TO 8
      SUM = SUM + DEGVAR(K)*PZ(K)
      GO TO 7
    8 CONTINUE
      SM(IPART,I) = SUM
      K = K + 1
      IF(IPART.GT.1) GO TO 6
    4 CONTINUE
C
      DO 9 IPART = 1,NN
      WRITE(LGOUT,75) N(IPART)
      WRITE(LGOUT,55)(SM(IPART,I),I = 1,NPSI)
    9 CONTINUE
      IF(IZ.LT.NPROB) GO TO 1
      STOP
C
    5 FORMAT(///)
   15 FORMAT(16I5)
   25 FORMAT(////,15X,11HPROBLEM NO.,I3)
   35 FORMAT(//,5X,46HINFLUENCE OF NEGLECTED DEGREES SUMMED UP TO N=,I3)
   45 FORMAT(//,5X,3HTHE,I3,27HVALUES OF PSI (DEGREES) ARE)
   55 FORMAT(8F10.3)
   65 FORMAT(//,5X,3HTHE,I3,38HVALUES OF INDIVIDUAL TRUNCATIONS N ARE)
   75 FORMAT(////,2X,50HEFECT (FOR GIVEN ANGLES PSI) OF THE TRUNCATION N =,I3,/)
      END
C
C
      SUBROUTINE LEGEN
      COMMON/ORDER/IORDER
      COMMON/COSPSI/ZED
      COMMON/PLEG/PZ(1000)
      DATA ONE, TWO/1.,2./
      PZ(1) = ZED
      PM2 = ONE
      PM1 = ZED
      DO 100 N = 2,IORDER
      XN = N
      VAR1 = ONE/XN
      VAR2 = TWO*XN-ONE
      VAR3 = XN - ONE
```

```
      B = VAR1*(ZED*VAR2*PM1 - VAR3*PM2)
      PZ(N) = B
      PM2 = PM1
      PM1 = B
100 CONTINUE
      RETURN
      END
```

APPENDIX 2

BEST LINEAR PREDICTION METHOD ON A GLOBAL SCALE

The development in this analysis follows closely that of [Heiskanen and Moritz, 1967], except that the matrix conventions are used throughout. It is based on the notion of covariance function as presented in Chapter 7 of this reference, which plays a fundamental role in the process of predictions (interpolations or extrapolations). Two remarks with regard to the adopted methodology are in order. First, the symbol E for mathematical expectation is replaced by M, indicating averages over the unit sphere as explained in the above reference. And second, the errors of the measurements themselves are considered to be zero. The errors, averages, etc., are associated exclusively with errors of prediction. Therefore, the "observations" play the role of errorless or theoretical quantities, which means that they equal their expected values. The predictions computed at points coinciding with "observation points" will be seen to be equal to the original observations and their error estimates (defined in terms of M-averages and not E-averages) will have values of exactly zero.
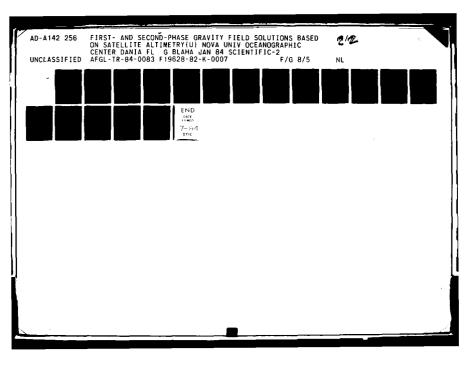
One can express all the observations, whose number is denoted by n, as the (column) vector F with n elements. For the present purpose, they will be considered as consisting of geoid undulations (little change in the derivations would occur if they consisted of gravity anomalies or other functions of the geopotential instead). The quantities to be predicted will be grouped in the vector $\hat{P}$ which represents an estimate of the vector P, containing unknown values of some function at arbitrarily chosen locations. This function may
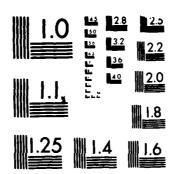
or may not be the same as the one observed, i.e., the one whose selected values are depicted by the elements of F. In fact, two kinds of functions will be considered herein in connection with the vector P: 1) geoid undulations as above, and 2) gravity anomalies. The prediction of P will be made possible through the known behavior of these geophysical quantities embodied in the covariance function (if P and F are of the same kind) or in the cross-covariance function (if P and F are of a different kind). It is to be emphasized that we are concerned here with the best linear prediction, in the sense that $\hat{P}$ consists of linear functions of the elements in F, and that the difference between $\hat{P}$ and P is minimized in a certain sense (upon using the operator M).

The pertinent covariance and cross-covariance functions are now described, starting with the surface spherical-harmonic expansion of gravity anomalies (Δg):

$$\Delta g = \sum_{n=2}^{\infty} \sum_{m=0}^{n} (\overline{c}_{nm} \cos m\lambda + \overline{d}_{nm} \sin m\lambda)\overline{P}_{nm}(\sin\phi) , \qquad (A2.1)$$

valid for the reference ellipsoid of the same mass and the same potential as the geoid; see [Heiskanen and Moritz, 1967], page 252 or the equation (7-13), etc. In this formula, ϕ and λ are the geocentric latitude and longitude of the point associated with Δg. The overbars indicate that the normalization has taken place (thus $\overline{P}_{nm}$ are the normalized associated Legendre functions). The relation between the coefficients in (A2.1) and the potential coefficients ($\overline{C}$'s and $\overline{S}$'s if normalized, C's and S's if conventional) is the following:

$$\left\{ \begin{array}{c} \overline{c}_{nm} \\ \overline{d}_{nm} \end{array} \right\} = G(n - 1) \left\{ \begin{array}{c} \Delta\overline{C}_{nm} \\ \Delta\overline{S}_{nm} \end{array} \right\}, \qquad (A2.2a)$$

-89-

MICROCOPY RESOLUTION TEST CHART

NATIONAL BUREAU OF STANDARDS-1963-A

where

$$\Delta\overline{C}_{n0} = \Delta C_{n0}/(2n+1)^{\frac{1}{2}} , \qquad (m=0) \tag{A2.2b}$$

$$\left\{\begin{array}{c} \Delta\overline{C}_{nm} \\ \\ \Delta\overline{S}_{nm} \end{array}\right\} = \{(n+m)!/[2(2n+1)(n-m)!]\}^{\frac{1}{2}} \left\{\begin{array}{c} \Delta C_{nm} \\ \\ \Delta S_{nm} \end{array}\right\} , \quad m>0 , \tag{A2.2c}$$

and where

ΔC_{n0} ... the correction to the reference C^*_{n0} in order to obtain C_{n0} ,

$$\left.\begin{array}{c} \Delta C_{nm} \equiv C_{nm} \\ \\ \Delta S_{nm} \equiv S_{n'} \end{array}\right\} \dots \text{ all the other coefficients },$$

G ... the average value of gravity.

It can be shown that the covariance function for gravity anomalies is

$$C(\psi) \equiv M\{\Delta g\ \Delta g'\} = \sum_{n=2}^{\infty} c_n\ P_n(\cos\psi) , \tag{A2.3}$$

where c_n , the degree variance for gravity anomalies, is

$$c_n \equiv M\{\Delta g_n^2\} = \sum_{m=0}^{n} (\overline{c}_{nm}^2 + \overline{d}_{nm}^2) = G^2(n-1)^2 \sum_{m=0}^{n} (\Delta\overline{C}_{nm}^2 + \Delta\overline{S}_{nm}^2) ,$$

and ψ is the spherical distance between the points associated with Δg and $\Delta g'$. Due to $P_n(\cos 0) \equiv 1$, one also has

$$C(0) \equiv M\{\Delta g^2\} = \sum_{n=2}^{\infty} c_n \equiv \sum_{n=2}^{\infty} M\{\Delta g_n^2\} . \tag{A2.3'}$$

Since usually $C_{20}=C_{20}^*$ and thus $\Delta C_{20}=0$, while $\Delta S_{n0}\equiv0$ for any n, then $c_2=0$ and the summations in (A2.3) and (A2.3') as well as in similar expressions below can start at n=3. These formulas therefore pertain to the "bandwidth" between n=3 and n=∞. If the reference gravity field were expressed through the degree n=n_1 (instead of 2 as is the case with the ellipsoidal field) the summations would start with n_1+1 (instead of 3). And if the complete field did not go beyond the degree n=n_2 the summations would end with n_2 (instead of ∞).

Under the same assumptions (equal mass and potential) as used in (A2.1), the geoid undulations (N) can be written as

$$N = (R/G) \sum_{n=2}^{\infty} [1/(n-1)] \sum_{m=0}^{n} (\overline{c}_{nm} \cos m\lambda + \overline{d}_{nm} \sin m\lambda)\overline{P}_{nm}(\sin\phi) , \quad (A2.4)$$

where R is the earth's mean radius. The covariance function for geoid undulations can similarly be derived as

$$D(\psi) \equiv M\{N\ N'\} = \sum_{n=2}^{\infty} d_n\ P_n(\cos\psi) , \quad\quad (A2.5)$$

where d_n , the degree variance for geoid undulations, is

$$d_n \equiv M\{N_n^2\} = \{R/[G(n-1)]\}^2\ c_n = R^2 \sum_{m=0}^{n} (\Delta\overline{C}_{nm}^2 + \Delta\overline{S}_{nm}^2) ;$$

from (A2.5) it follows that

$$D(0) \equiv M\{N^2\} = \sum_{n=2}^{\infty} d_n \equiv \sum_{n=2}^{\infty} M\{N_n^2\} . \quad\quad (A2.5')$$

The cross-covariance function for gravity anomalies and geoid undulations can be obtained as

$$H(\psi) \equiv M\{\Delta g \ N'\} \equiv M\{N \ \Delta g'\} = \sum_{n=2}^{\infty} h_n \ P_n(\cos\psi) \ , \qquad (A2.6)$$

where

$$h_n = \{R/[G(n-1)]\}c_n = [G(n-1)/R]d_n = RG(n-1) \sum_{m=0}^{n} (\Delta \overline{C}_{nm}^2 + \Delta \overline{S}_{nm}^2) \ ,$$

$$h_n \equiv M\{\Delta g_n \ N_n\} \equiv M\{N_n \ \Delta g_n\} \ ;$$

one also has

$$H(0) = \sum_{n=2}^{\infty} h_n \ , \qquad (A2.6')$$

or

$$H(0) \equiv M\{\Delta g \ N\} \equiv M\{N \ \Delta g\} = \sum_{n=2}^{\infty} M\{\Delta g_n \ N_n\} \equiv \sum_{n=2}^{\infty} M\{N_n \ \Delta g_n\} \ .$$

Attention may now be focused on finding the best linear estimates $\hat{P}$,

$$\hat{P} = A^T F \ . \qquad (A2.7)$$

(This formulation resembles superficially the usual prediction formula in stochastic processes; however, the latter notion involves the expectation operator E and permits $\Sigma_F \neq 0$, unlike the present approach.) The matrix A^T contains as yet unknown constants. The problem of finding A^T is addressed through the M operator. We first form a "dispersion matrix", where $\varepsilon \equiv P - \hat{P}$, as follows:

$$\varepsilon\varepsilon^T \equiv (P - A^T F)(P - A^T F)^T = PP^T - PF^T A - A^T FP^T + A^T FF^T A \ ; \qquad (A2.8)$$

-92-

its average over the unit sphere is

$$M\{\varepsilon\varepsilon^T\} = M\{PP^T\} - M\{PF^T\}A - A^TM\{FP^T\} + A^TM\{FF^T\}A . \tag{A2.9}$$

Although PP^T, PF^T, FP^T are unknown, the global means of these values, $M\{PP^T\}$, $M\{PF^T\}$, $M\{FP^T\}$ are known from the variance (and cross-covariance) function.

Next we stipulate that the matrix $M\{\varepsilon\varepsilon^T\}$ should have a minimum trace, thus applying the operator "Tr" and differentiating with respect to A^T; the result has to equal the zero matrix, namely

$$\partial Tr[M\{PP^T\}]/\partial A^T - 2 \; \partial Tr[A^TM\{FP^T\}]/\partial A^T + \partial Tr[A^TM\{FF^T\}A]/\partial A^T = 0 ,$$

where use was made of $Tr[B] = Tr[B^T]$. Applying the rules for differentiation of traces (see e.g. [Blaha, 1976], pages 12 and 13) one obtains

$$0 - 2 \; M\{PF^T\} + 2 \; A^TM\{FF^T\} = 0 ,$$

and thus

$$A^T = M\{PF^T\}[M\{FF^T\}]^{-1} . \tag{A2.10}$$

The estimate $\hat{P}$ is then given from (A2.7) as

$$\hat{P} = M\{PF^T\}[M\{FF^T\}]^{-1}F . \tag{A2.11}$$

If (A2.10) is substituted into (A2.9), the second, third and fourth matrices on the right-hand side become equal and the result is

$$M\{\varepsilon\varepsilon^T\} = M\{PP^T\} - M\{PF^T\}[M\{FF^T\}]^{-1}M\{FP^T\} . \tag{A2.12}$$

The relations (A2.10-12) are now written as

$$A^T = M^T H^{-1} , \qquad\qquad\qquad (A2.10')$$

$$\hat{P} = M^T H^{-1} F = M^T W , \qquad\qquad\qquad (A2.11')$$

$$M\{\epsilon\epsilon^T\} = H_p - M^T H^{-1} M , \qquad\qquad\qquad (A2.12')$$

with the use of the following notations:

$$W \equiv H^{-1} F ;$$

$$H \equiv M\{FF^T\} ;$$

$$M^T \equiv M\{PF^T\} , \qquad H_p \equiv M\{PP^T\} .$$

The matrices M, H should not be confused with the operator M{} and the cross-covariance function H(ψ), respectively. All of the above notations may be used when the functions in P and in F are of the same kind (here geoid undulations).

When these functions are of a different kind (gravity anomalies associated with P, geoid undulations associated with F as above), all the matrices and vectors may be identified by the symbol "~" except F, H, W which remain the same. We can thus write

$$\tilde{A}^T = \tilde{M}^T H^{-1} , \qquad\qquad\qquad (A2.10'')$$

$$\hat{\tilde{P}} = \tilde{M}^T H^{-1} F = \tilde{M}^T W , \qquad\qquad\qquad (A2.11'')$$

$$M\{\tilde{\epsilon}\tilde{\epsilon}^T\} = H_{\tilde{p}} - \tilde{M}^T H^{-1} \tilde{M} . \qquad\qquad\qquad (A2.12'')$$

-94-

The formula (A2.11") is interesting in that only the matrix $\tilde{M}^T$ changes (it is now computed using the cross-covariance function), while the vector $W \equiv H^{-1}F$ is the same whether $\hat{P}$ or $\hat{\hat{P}}$ are sought. This procedure can be referred to as a best prediction of gravity anomalies from geoid undulations (errorless values as stipulated).

The matrix A^T (or $\tilde{A}^T$) in all previous formulas was found subject to the condition that the M-average of all the diagonal elements in $\varepsilon\varepsilon^T$ be simultaneously as small as possible. In considering only one prediction point, P, $\hat{P}$, ε comprise each only one element and A^T, $M\{PF^T\}$ in (A2.9) consist each of only one row as a special case. The derivation would then become somewhat simpler in that the operator Tr would be omitted. In fact, after the transposition of the third term (a 1x1 matrix) on the right-hand side of (A2.9) and the differentiation of the whole expression with respect to the vector A, one would recover the equation preceding (A2.10). The row vector A^T in (A2.10), etc., would now correspond to one minimum element $M\{\varepsilon^2\}$.

The matrices H, M^T and $\tilde{M}^T$ will now be expressed more explicitly. For the sake of clarity, the observation points will be identified with numbers or small-letter indices while the prediction points will be identified with capital-letter indices. The matrix H can be written as

$$H \equiv M\{FF^T\} = \begin{bmatrix} D_o & D_{12} & \cdots & D_{1n} \\ & D_o & \cdots & D_{2n} \\ \text{symm.} & & & \vdots \\ & & & D_o \end{bmatrix}, \tag{A2.13}$$

where $D_o \equiv D(0)$ and $D_{ij} \equiv D(\psi_{ij})$, and where n, the number of observation points, need not be confused with the same symbol used earlier to denote the degree in a spherical-harmonic expansion. The matrix M^T is represented as follows:

$$M^T \equiv M\{PF^T\} = \begin{bmatrix} & \vdots & \\ D_{J1} & D_{J2} & \cdots & D_{Jn} \\ & \vdots & \\ D_{L1} & D_{L2} & \cdots & D_{Ln} \\ & \vdots & \end{bmatrix}, \tag{A2.14}$$

while the matrix $\tilde{M}^T$ is

$$\tilde{M}^T \equiv M\{\tilde{P}F^T\} = \begin{bmatrix} & \vdots & \\ H_{J1} & H_{J2} & \cdots & H_{Jn} \\ & \vdots & \\ H_{L1} & H_{L2} & \cdots & H_{Ln} \\ & \vdots & \end{bmatrix}. \tag{A2.15}$$

The matrix $H_p \equiv M\{PP^T\}$ in (A2.12') has a structure similar to (A2.13) above, except that i,j now correspond to the predicted points. And the matrix $H_{\tilde{p}} \equiv M\{\tilde{P}\tilde{P}^T\}$ in (A2.12") would be constructed as H_p (i.e., using predicted points), except that the covariance function "D" would be replaced by the covariance function "C" seen earlier.

Suppose now that the point J in (A2.14) coincides with one point of F, e.g. with the i-th point. The row corresponding to this point in M^T then becomes $[D_{i1} \quad D_{i2} \quad \cdots \quad D_o \quad \cdots \quad D_{in}]$, identical to the i-th row in H. When the

multiplication in (A2.10) or (A2.10') is performed, the pertinent row in A^T contains zeros everywhere except at its i-th place where it contains +1. One thus has for the prediction (A2.11) or (A2.11'):

$$
\hat{P} \equiv \begin{bmatrix} \vdots \\ \hat{P}_J \\ \vdots \end{bmatrix} = \begin{bmatrix} & & \vdots & & \\ 0 \ldots 0 & 1 & 0 & \ldots & 0 \\ & & \vdots & & \end{bmatrix} \begin{bmatrix} F_1 \\ \vdots \\ F_{i-1} \\ F_i \\ F_{i+1} \\ \vdots \\ F_n \end{bmatrix} ,
$$

and

$$
\hat{P}_J = F_i ,
$$

i.e., the prediction coincides with the (errorless) observation. The same argument may be repeated when all the predicted points coincide with the n observation points, in which case

$$
M^T \equiv H ,
$$

$$
\hat{P} = M^T H^{-1} F \equiv F ,
$$

so that all the predictions coincide with the observations.

The situation with respect to $M\{\varepsilon\varepsilon^T\}$ in (A2.12) or (A2.12') is examined next. The diagonal of H_P contains D_o values everywhere. When the point J coincides with the i-th point in F, the pertinent row in $M^T H^{-1}$ again has zeros

everywhere, except for +1 at its i-th place. The corresponding column (for the point J) in M has the form $\begin{bmatrix} D_{i1} & D_{i2} & ... & D_o & ... & D_{in} \end{bmatrix}^T$ seen before in the transposed form; the element D_o appears at the i-th place. Thus, the element of $M^T H^{-1} M$ at the location (i,i) is D_o from which it follows that

$$M\{\varepsilon_J^2\} = D_o - D_o \equiv 0 .$$

If again all the predicted points coincide with the n observation points, we see immediately that

$$H_P \equiv H ,$$

and, as above,

$$M^T \equiv H ;$$

accordingly,

$$M\{\varepsilon\varepsilon^T\} = H - HH^{-1}H^T \equiv 0 .$$

Thus the average dispersion matrix is zero, which could be loosely termed as "perfect prediction". It is prudent to refrain from calling the diagonal elements in $M\{\varepsilon\varepsilon^T\}$ as variances and the off-diagonal elements as covariances, since in statistics such a terminology is customarily associated with random variables (rather than with some theoretical function values) and with the operator E.

In summary, the theoretical (errorless) values of some function (here geoid undulations) at several discrete points are used to make a linear

prediction of the same function, or a different function (here gravity anomalies), at arbitrarily chosen locations. This is possible solely due to the knowledge of behavior of these geophysical quantities, embodied in the covariance and cross-covariance functions; these functions are obtained through a stationary process on the (unit) sphere and are ultimately given in terms of the spherical-harmonic (S.H.) potential coefficients. An important property of this approach is that the prediction at an observation point yields the observation itself (here an errorless quantity) with the zero prediction error. At other points the predictions are optimized in the sense that they result in the smallest trace of the dispersion matrix obtained using the M-averaging.

In practice, the covariance function may be computed from some approximate values of the S.H. coefficients complete through a certain degree and order. It can be argued that this function should be compatible with the observations and should ideally be computed from them, since it seems only reasonable to assume that if one is making predictions which are based on some measured values, the covariance function should be closely related to them. However, it is quite possible that the predicted values are relatively insensitive to variations in the covariance function. Be that as it may, caution should be exercised when interpreting the predicted values and certain prediction errors represented by $M\{\varepsilon\varepsilon^T\}$. The covariance function as used in these computations expresses a general behavior of the theoretical function with respect to its whole domain, the earth. Therefore, individual predictions may be somewhat "blurred" by this global property, while being "best" overall. This "blurring" effect is even more noticeable when the average matrix $M\{\varepsilon\varepsilon^T\}$

is considered, since ϵ is expressed in terms of A^T which already depends on the covariance function and, further, since the product $\epsilon\epsilon^T$ is averaged over the whole earth.

An important practical advantage of the best linear prediction method resides in avoiding inversions of large matrices. For the price of introducing certain (admissible) errors, only a small number of observations may be used to predict a function at any desired location. The observation points included should be chosen in the neighborhood of the prediction poi   The size of the neighborhood and the number (n) of observation points   subject to judgment. The matrix H to be inverted, then, has the dimensions $(n \times n)$ and most often is likely to be comfortably small. This feature is attributed to the fact that the covariance functions considered decrease rather rapidly with increasing distances from prediction points since geoid undulations and, especially, gravity anomalies are most affected by local and regional factors.

APPENDIX 3

TRANSLOCATION ALGORITHM ADAPTED FOR THE
LEAST-SQUARES COLLOCATION WITH NOISE

In reference to Section 6.4, the task at hand can be presented as follows. Given the prediction point J and two observation points numbered for convenience 1 and 2, find the seven values of the "storage" matrix for the averaged point P replacing both of the original observation points. These points are considered to be averaged for the first time so that their weights are taken as

$$p_1 = 1/\psi_{J1} , \qquad p_2 = 1/\psi_{J2} . \tag{A3.1a,b}$$

If they were computed, the coordinates (ϕ, λ) of P would be given by

$$\phi = (p_1\phi_1 + p_2\phi_2)/(p_1 + p_2) , \quad \lambda = (p_1\lambda_1 + p_2\lambda_2)/(p_1 + p_2) ; \tag{A3.2a,b}$$

the corresponding value of the geoid undulation at P is

$$N = (p_1 N_1 + p_2 N_2)/(p_1 + p_2) . \tag{A3.3}$$

If one denotes

$$d\phi = \phi_2 - \phi_1 , \qquad d\lambda = \lambda_2 - \lambda_1 , \tag{A3.4a,b}$$

it follows from (A3.2a,b) that

$$\tag{A3.5a,b,c}$$

$$d\phi_1 \equiv \phi - \phi_1 = w \, d\phi , \quad d\lambda_1 \equiv \lambda - \lambda_1 = w \, d\lambda , \quad w = p_2/(p_1 + p_2) .$$

In fact, upon considering a (small) rectangular triangle formed, on a unit sphere, by the segment of the great circle between 1 and 2 and by the corresponding segments of one meridian and one parallel, one would also deduce

$$d\phi_1/d\phi_2 = d\lambda_1/d\lambda_2 = \psi'/\psi'' = p_2/p_1 = \psi_{J1}/\psi_{J2} \; ,$$

where $d\phi_2 = \phi_2 - \phi$, $d\lambda_2 = \lambda_2 - \lambda$ and ψ' , ψ'' are the angular distances 1-P and P-2, respectively, measured along 1-2. In other words, $\psi'/\psi'' = \psi_{J1}/\psi_{J2}$ gives the location of P with respect to the locations of 1 and 2 according to the desired emphasis on the distances of the observation points 1 and 2 from the prediction point J.

Next designate ϕ_1 or λ_1 by the general symbol α_1, ϕ_2 or λ_2 by the general symbol α_2, and ϕ or λ by the general symbol α. Consider the most conservative case when dealing with round-off errors and their dependence on α_1 and include second-order effects so that the error is of the order $(\alpha_2 - \alpha_1)^3$ at the most. Upon applying the first parts of (A3.5a,b) to "α", one has

$$\sin\alpha = \sin\alpha_1 + \cos\alpha_1 d\alpha_1 - \frac{1}{2} \sin\alpha_1 d\alpha_1^2 \; , \tag{A3.6a}$$

$$\cos\alpha = \cos\alpha_1 - \sin\alpha_1 d\alpha_1 - \frac{1}{2} \cos\alpha_1 d\alpha_1^2 \; . \tag{A3.6b}$$

The following relations, which should be understood as approximations to within the desired accuracy, will be used:

$$d\alpha^2 = (\sin\alpha_2 - \sin\alpha_1)^2/\cos^2\alpha_1 \; \dots \; \text{if } |\cos\alpha_1| \geq |\sin\alpha_1| \; , \tag{A3.7a}$$

$$d\alpha^2 = (\cos\alpha_2 - \cos\alpha_1)^2/\sin^2\alpha_1 \; \dots \; \text{if } |\cos\alpha_1| < |\sin\alpha_1| \; . \tag{A3.7b}$$

The above distinction with regard to α_1 gives rise to the cases "a" and "b" in the same order.

If (A3.4a,b) are applied to "α", one obtains (A3.6a,b) with α_2 replacing α and $d\alpha$ replacing $d\alpha_1$. From these new equations, respectively, and from (A3.7a,b), respectively, it then follows for the cases a and b:

$$d\alpha = T_1(1 + \tfrac{1}{2}tg\alpha_1 \times T_1) , \qquad T_1 = (sin\alpha_2 - sin\alpha_1)/cos\alpha_1 , \qquad \text{(A3.8a)}$$

$$d\alpha = -T_1'(1 + \tfrac{1}{2}cotg\alpha_1 \times T_1') , \qquad T_1' = (cos\alpha_2 - cos\alpha_1)/sin\alpha_1 . \qquad \text{(A3.8b)}$$

The second parts of (A3.5a,b) applied to "α" yield

$$d\alpha_1 = w\, d\alpha , \qquad d\alpha_1^2 = w^2 d\alpha^2 ,$$

where w is given in (A3.5c), $d\alpha$ is given in (A3.8a) or (A3.8b), and $d\alpha^2$ is adopted from (A3.7a) or (A3.7b). With these quantities, equations (A3.6a,b) are readily transcribed as

$$\text{(A3.9a)}$$
$$sin\alpha = sin\alpha_1 + T_2 cos\alpha_1 - \tfrac{1}{2}T^2 sin\alpha_1 , \quad T = w\, T_1 , \quad T_2 = T(1 + \tfrac{1}{2}T_1 tg\alpha_1) ;$$

$$\text{(A3.9b)}$$
$$cos\alpha = cos\alpha_1 + T_2' sin\alpha_1 - \tfrac{1}{2}T'^2 cos\alpha_1 , \quad T' = w\, T_1' , \quad T_2' = T'(1 + \tfrac{1}{2}T_1' cotg\alpha_1) .$$

The algorithm can now be summarized.

If $|\cos\alpha_1| \geq |\sin\alpha_1|$:

$$\sin\alpha = \sin\alpha_1 + T_2\cos\alpha_1 - \frac{1}{2}T^2\sin\alpha_1 \; ;$$

$$\cos\alpha = \pm(1 - \sin^2\alpha)^{\frac{1}{2}} \; , \quad \text{sign}(\cos\alpha) = \text{sign}(\cos\alpha_1) \; ;$$

$$T_1 = (\sin\alpha_2 - \sin\alpha_1)/\cos\alpha_1 \; , \quad T = w\,T_1 \; , \quad T_2 = T(1 + \frac{1}{2}T_1\sin\alpha_1/\cos\alpha_1) \; .$$

If $|\cos\alpha_1| < |\sin\alpha_1|$:

$$\cos\alpha = \cos\alpha_1 + T_2'\sin\alpha_1 - \frac{1}{2}T'^2\cos\alpha_1 \; ;$$

$$\sin\alpha = \pm(1 - \cos^2\alpha)^{\frac{1}{2}} \; , \quad \text{sign}(\sin\alpha) = \text{sign}(\sin\alpha_1) \; ;$$

$$T_1' = (\cos\alpha_2 - \cos\alpha_1)/\sin\alpha_1 \; , \quad T' = w\,T_1' \; , \quad T_2' = T'(1 + \frac{1}{2}T_1'\cos\alpha_1/\sin\alpha_1) \; .$$

$$N = (p_1 N_1 + p_2 N_2)/(p_1 + p_2) \; .$$

The quantity w is given in (A3.5c) while p_1 and p_2 are given in (A3.1a,b), respectively. As stipulated, only sine and cosine functions (needed in the "storage" matrix of Section 6.4) appear in this algorithm. With regard to the angles "ψ", these functions are computed by the standard formulas.

REFERENCES

Blaha, G., The Least Squares Collocation from the Adjustment Point of View and Related Topics. AFGL Technical Report No. 76-0073, Air Force Geophysics Laboratory, Hanscom AFB, Massachusetts, 1976; ADA024203.

Blaha, G., SEASAT Altimetry Adjustment Model Including Tidal and Other Sea Surface Effects. AFGL Technical Report No. 81-0152, Air Force Geophysics Laboratory, Hanscom AFB, Massachusetts, 1981; ADA104188.

Blaha, G., Modeling and Adjusting Global Ocean Tides Using SEASAT Altimeter Data. AFGL Technical Report No. 82-0114, Air Force Geophysics Laboratory, Hanscom AFB, Massachusetts, 1982; ADA115841.

Blaha, G., Point-Mass Modeling of the Gravity Field with Emphasis on the Oceanic Geoid. AFGL Technical Report No. 83-0007, Air Force Geophysics Laboratory, Hanscom AFB, Massachusetts, 1983; ADA130535.

Brown, D.C. and J. E. Trotter, SAGA, a Computer Program for Short Arc Geodetic Adjustment of Satellite Observations. DBA Systems, Inc., P.O. Drawer 550, Melbourne, Florida, 1969.

Estes, R.H., "A Simulation of Global Ocean Tide Recovery Using Altimeter Data with Systematic Orbit Error". Paper published in Marine Geodesy, Volume 3, Nos. 1-4, Crane Russak, New York, 1980.

Heiskanen, W.A. and H. Moritz , Physical Geodesy. W.H. Freeman and Co., San Francisco, 1967.

Hess, S.L., Introduction to Theoretical Meteorology. Holt, Rinehart and Winston, New York, 1959.

Hotine, M., Mathematical Geodesy. Monogr. Ser., Vol. 2, Environ. Sci. Serv. Admin., Washington, D.C., 1969.

Kautzleben, H. and F. Barthelmes, "Point Mass-Representation of the Earth's Gravity Field". Paper published in the Proceedings of the International Symposium: Figure of the Earth, the Moon and Other Planets, printed by the Research Institute of Geodesy, Topography and Cartography, Prague, Czechoslovakia, 1983.

Moritz, H., Advanced Physical Geodesy. Abacus Press, Turnbridge Wells Kent, Great Britain, 1980.

Parke, M.E. and M.C. Hendershott, "M2, S2, K1 Models of the Global Ocean Tide on an Elastic Earth". Paper published in Marine Geodesy, Volume 3, Nos. 1-4, Crane Russak, New York, 1980.

Tscherning, C.C. and R.H. Rapp, Closed Covariance Expressions for Gravity Anomalies, Geoid Undulations, and Deflections of the Vertical Implied by Anomaly Degree Variance Models. Report No. 208, Department of Geodetic Science, The Ohio State University, Columbus, 1974.

Schwiderski, E.W., "Ocean Tides, Part I: Global Ocean Tidal Equations". Paper published in Marine Geodesy, Volume 3, Nos. 1-4, Crane Russak, New York, 1980.